Audit of the global carbon budget: estimate errors and their impact on uptake uncertainty

Ballantyne AP [1], Andres R [2], Houghton R [3], Stocker BD [4], Wanninkhof R [5], Anderegg W [6], Cooper LA[1], DeGrandpre M[1], Tans PP[7], Miller JC[7], Alden C[8], White JWC[9]

[1] University of Montana, Missoula, MT, USA

[2] Carbon Dioxide Information Analysis Center, Oak Ridge National Laboratory, TN, USA

[3] Woods Hole Research Center, Falmouth, MA, USA

[4] Imperial College, London, UK

[5]Atlantic Oceanographic and Meteorological Laboratory of NOAA, Miami, FL, USA

[6]Princeton Environmental Institute, Princeton University, Princeton, NJ, USA

[7]Earth System Research Laboratory of NOAA, Boulder, CO, USA

[8]Stanford University, Palo Alto, CA, USA

[9]Institute Alpine and Arctic Research, CU Boulder, CO, USA

Correspondence email: ashley.ballantyne@umontana.edu

Abstract:

Over the last 5 decades monitoring systems have been developed to detect changes in the accumulation of carbon (C) in the atmosphere and ocean; however, our ability to detect changes in the behavior of the global C cycle is still hindered by measurement and estimate errors. Here we present a rigorous and flexible framework for assessing the temporal and spatial components of estimate error and their impact on uncertainty in net C uptake by the biosphere. We present a novel approach for incorporating temporally correlated random error into the error structure of emission estimates. Based on this approach, we conclude that the 2 σ errors of the atmospheric growth rate have decreased from 1.2 PgC yr^{-1} in the 1960s to 0.3 PgC yr^{-1} in the 2000s due to an expansion of the atmospheric observation network. The 2 σ errors in fossil fuel emissions have increased from 0.3 PgC yr^{-1} in the 1960s to almost 1.0 PgC yr^{-1} during the 2000s due to differences in national reporting errors and differences in energy inventories. Lastly, while land use emissions have remained fairly constant, their errors still contribute substantially to global C uptake uncertainty. Currently, the absolute errors in fossil fuel emissions rival the total emissions from land use, highlighting the extent to which fossil fuels dominate the global C budget. Because errors in the atmospheric growth rate have decreased faster than errors in total emissions have increased, a ~20% reduction in the over-all uncertainty of net C global uptake has occurred. Given all the major sources of error in the global C budget that we could identify, we are 93% confident that terrestrial C uptake has increased and 97% confident that ocean C uptake has increased over the last 5 decades. Thus it is clear that arguably one of the most vital ecosystem services currently provided by the biosphere is the continued removal of approximately half of atmospheric CO_2 emissions from the atmosphere; although, there are certain environmental costs associated with this service, such as the acidification of ocean waters.

1.0 Introduction: incorporating error into the global carbon budget

Remarkable progress has been made in the study of the global carbon (C) budget over the last 50 years; however, errors associated with CO_2 measurements and emission estimates still limit our confidence in calculating net C uptake from the atmosphere by the land and ocean. Since the first continuous measurements of atmospheric CO_2 at Mauna Loa were started in 1959 (Keeling et al., 2011), the global network of continuous monitoring sites has expanded to over 300 sites and continues to grow (Global View-CO2, 2013). This expansion of the monitoring network allows us to resolve spatial patterns associated with the seasonal uptake and release of CO_2 from and to the atmosphere at an unprecedented scale. Similarly nearly 10 million measurements of partial pressure of CO_2 (pCO_2) have been made in the world's oceans since 1957 (Bakker et al., 2014; Takahashi et al., 2014) allowing us to estimate CO_2 uptake by the oceans. From global measurements of CO_2 and its isotopic composition, it is clear that C emitted from industrial activities (Boden et al., 2009) and human land use (Houghton, 1995) have led to the accumulation of CO_2 in the atmosphere and pCO_2 in the oceans.

Even though our understanding of the global C cycle has benefited tremendously from this unprecedented global C monitoring network, we continue to struggle with errors in our measurements and estimates of terms in the global C budget that limit our ability to draw confident conclusions regarding changes in net C uptake by the biosphere. As we enter into an era in which scientists are expected to provide an increasingly more detailed assessment of carbon uptake at increasingly higher spatial and temporal resolutions (Canadell et al., 2011), it is critical that we develop a framework for the incorporation and propagation of spatial and temporal errors into our calculations to prioritize future research efforts. Furthermore, it is imperative that explicit uncertainties in the global carbon budget be made available to policy makers so that our best estimates can be weighted by levels of uncertainty such that the most informed policy decisions can be made.

The objective of this synthesis is to identify the major sources of error in the important terms of the global C budget and to assess how these errors affect calculations of net global C uptake by the biosphere and partitioning of uptake between land and ocean sinks. Although this is an attempt to fully incorporate errors into global C cycle analyses, we acknowledge that there are latent sources of error that remain unknown and are difficult to incorporate into our analysis at this time. However, the framework that we develop here for incorporating both the spatial and temporal error structure is flexible and can be used to incorporate additional sources of error as our knowledge of the global C budget progresses. The ultimate goal of this analysis is to identify and incorporate all known sources of error into the global C budget and provide conclusions with confidence intervals of changes in C uptake over the observational period from 1959 to 2010.

1.1 Important terms of the global carbon budget

Prior to identifying the main sources of error in the global carbon budget, it is necessary to describe the key processes controlling changes in atmospheric CO_2 concentrations. According to the mass balance of the atmosphere:

$$\frac{dC}{dt} = E_F + E_L + N_O + N_L \quad . \quad (1)$$

Where $\frac{dC}{dt}$ represents the annual growth rate of atmospheric CO_2, E_F represents the one-way flux of fossil fuel emissions, including cement production, to the atmosphere (Andres et al., 2012), and E_L represents land use emissions to the atmosphere (Houghton et al., 2012). Atmospheric CO_2 is constantly being exchanged between the atmosphere and the biosphere, where N_L represents net C exchange by the land through photosynthesis and respiration and N_O represents net C exchange by the ocean through air-sea gas exchange. Although land use emission estimates were originally derived to capture C emissions as a result of clearing primary forest, the operational definition of E_L has expanded to include deforestation and processes affecting forest regrowth, such as CO_2 fertilization and N deposition (Houghton et al., 2012). These different processes incorporated into the E_L term are difficult to disentangle and quantify at the global scale and thus their combined uncertainty is considered in our error analysis. Because we have defined the global C budget with respect to the atmosphere, all emission terms (*E*) add C to the atmosphere and thus have a positive sign, whereas the net exchange terms (*N*) can have a negative sign indicating net C uptake from the atmosphere or a positive sign indicating net C release to the atmosphere. All of the terms in the budget can be measured directly or estimated on an annual time step, except the net land uptake term (i.e. N_L) that is inferred as the residual land C sink. Thus here we consider the statistical error associated with the measurement (e.g. CO_2) or estimates (e.g. E_F and E_L) of each term in the global C budget (see Eq1 and Fig. 1).

Below, we provide a brief overview of the sources of error in measurement of growth of atmospheric CO_2 and each of the terms in the carbon budget. We then construct a global carbon budget with a full accounting and propagation of error using a Monte Carlo type approach. To separate ocean and land uptake we rely on ocean models constrained by observations. We conclude with a discussion of the important sources of error and their impact on uncertainties in calculating land and ocean C uptake.

1.2 Sources of error in atmospheric CO_2 measurements

Most of the error associated with measuring annual changes in atmospheric CO_2 (i.e. $\frac{dC}{dt}$) at the global scale is not due to instrumental accuracy or precision, but rather due to the location and number of sampling sites at which atmospheric CO_2 measurements are made (Conway et al., 1994). Until recently, measurements of atmospheric CO_2 have been made primarily using infrared gas analyzers that have a reported accuracy of 0.3 ppm, reproducibility of 0.5 ppm, and precision of approximately 0.05 ppm (Conway et al., 1994; Keeling, 1960). However, because measurements of atmospheric CO_2 are made across a spatially heterogeneous network of sites, errors in quantifying changes in atmospheric concentration of CO_2 may occur. Although it is possible to control for local contamination by only using background sites located within the marine boundary layer, errors still arise as a result of where atmospheric CO_2 measurements are made. As the atmospheric growth rate of CO_2 has increased, the uncertainty in the growth rate has gone down due to the addition of sampling sites to the global CO_2 observing network. Although recent advances in laser technology have greatly increased the precision and frequency of gas phase CO_2 measurements, ultimately our ability to resolve changes in atmospheric

CO_2 concentration and attribute them to regional fluxes may still be limited by the spatial distribution of sites in the global CO_2 observatory.

1.3 Sources of error in oceanic pCO_2 measurements

Just as there are errors associated with CO_2 measurements made in the atmosphere, there are also errors associated with pCO_2 measurements made in the ocean. Ocean C uptake is estimated as a function of the gradient in partial pressure between the atmosphere and the ocean ($\Delta\ pCO_2$), as well as the kinetics of CO_2 gas transfer and solubility. Uncertainty in net ocean C uptake is most sensitive to errors in the long term pCO_2 trend, but other factors such as wind speed and sea surface temperature that affect the kinetics of air-sea gas exchange may also be important (Wanninkhof et al., 2013). The partial pressure of CO_2 in the ocean is much more variable than in the overlying atmosphere. Because pCO_2 values vary by as much as 100 µatm on seasonal to interannual timescales and become spatially uncorrelated at 10^2 km, extrapolating pCO_2 values is statistically challenging (Li et al., 2005). Although statistical techniques for extrapolating pCO_2 and estimating C uptake by the oceans are improving (e.g. Landschützer et al., 2013; Rödenbeck et al., 2013), researchers often rely on ocean biogeochemical models to expand inference to the global scale (Le Quéré et al., 2013; Le Quéré et al., 2010). The largest uncertainty in estimating net global exchange of CO_2 between the ocean and the atmosphere is due to the assumption that pCO_2 in the ocean changes at the same rate as pCO_2 in the atmosphere, leading to a time invariant $\Delta\ pCO_2$. However, studies suggest that $\Delta\ pCO_2$ is not constant and may have decreased in recent decades in the North Atlantic resulting in decreased C uptake (Schuster and Watson, 2007) and may have increased recently in the Pacific resulting in increased C uptake (Le Quéré et al., 2010). Difficulties also arise in extrapolating estimates of ocean C uptake to the Southern Hemisphere where observational constraints on simulations are sparse (Lenton et al., 2013) and in coastal regions that may be affected by continental delivery of dissolved inorganic C or complex upwelling patterns (Dai et al., 2013). The overall 2 σ uncertainty in C uptake by the ocean has been estimated empirically from atmospheric O_2 to be between 1.2 and 1.4 PgC yr^{-1} (Ishidoya et al., 2012; Manning and Keeling, 2006) which is slightly higher than the 2 σ uncertainty of 1.0 PgC yr^{-1} based on estimates from ocean biogeochemical models (Le Quéré et al., 2013).

1.4 Sources of error in estimating fossil fuel emissions

The greatest contributor to the increase in atmospheric CO_2 over the last 50 years is emissions from the combustion of fossil fuels and cement production (E_F) and therefore errors associated with these emissions have the potential to result in large uncertainties in the global C budget. Global emissions of fossil fuels have increased significantly during the last 5 decades, but relative errors of fossil fuel emission estimates have also increased leading to a substantial increase in absolute errors in fossil fuel emissions (Ballantyne et al. 2012). Although our understanding of sources of error in fossil fuel emission estimates has greatly improved, emissions are increasing faster in nations with less accurate emission estimates thus leading to an increase in both relative and absolute errors of global fossil fuel emissions (Andres et al., 2014b; Andres et al., 2012). Because fossil fuel emissions are often estimated from energy consumption or production statistics, they are a fairly well constrained economic variable.

Nonetheless, there are two primary sources of error that lead to uncertainties among and within fossil fuel emission inventories.

First, methodological differences in how energy consumption statistics are converted to CO_2 emissions may lead to different fossil fuel emission estimates among different inventories. Most global fossil fuel inventories include emission estimates from solid, liquid, and gas fossil fuels, but the emission coefficients used to convert fossil fuel consumption to CO_2 emissions may vary among inventories (Andres et al., 2012). Furthermore, fossil fuel inventories may also differ in their inclusion or treatment of estimated emissions from cement production, gas flaring, and bunker fuels used for international transport. These slight differences in how inventories treat industrial emissions can lead to significant differences in estimates among inventories. While the slightly different methodological approaches employed by different inventories provide useful independent estimates of fossil fuel emissions, these independent estimates contribute to the global fossil fuel emission uncertainty.

The second major source of error in fossil fuel emission estimates is due to emission accounting practices of individual countries. It has long been suspected that emission reporting practices of developing nations are less reliable than reporting practices from developed nations (Marland et al., 2009). Another important characteristic of the error structure in emission estimates is that some components of the emission errors may be temporally correlated from year to year (Ballantyne et al., 2012; Marland et al., 2009). The global 2σ relative error on the flux weighted fossil fuel emission estimates is thought to range between 5 and 10%. Thus it is clear that slight discrepancies in fossil fuel emission estimates may lead to potentially large impacts on inferred global C uptake (Francey et al., 2013).

1.5 Sources of error in estimating land use change emissions

Although emissions from changes in land use and land cover (i.e. E_L) contribute a smaller fraction to total emissions of atmospheric CO_2, there are considerable errors in estimating CO_2 emissions from land use change and thus errors in land use emission estimates can result in large uncertainties in carbon uptake estimates. In the 1950s approximately 30% of total CO_2 emissions to the atmosphere were from land use change compared to the last decade in which only 10% of the total emissions were from land use change. This reduction in the fraction of emissions due to land use change is largely the result of significant increases in fossil fuel emissions combined with nearly constant land-use emissions over the last 50 years (Houghton et al., 2012). There are two different approaches to estimating emissions from changing patterns in land-use and land-cover change (LULCC): bookkeeping and process-based models.

Bookkeeping techniques involve integrating either census or satellite data on forestry and agriculture with data on carbon densities to calculate sources and sinks of carbon based on empirical models (DeFries et al., 1999; Houghton, 1995). The second approach uses process-based ecosystem models to estimate carbon densities and rates of change in these densities as a result of the same drivers of LULCC (i.e, forestry and agriculture) (Stocker et al., 2011; Yang et al., 2010). The major difference between these two approaches is that process-based models include the effects of environmental change (e.g., CO_2, climate, N deposition) on rates of decomposition and growth, while in the bookkeeping approach

these rates are constant through time. Each of these approaches attempts to capture the net effect of C release from deforestation and C uptake in forest regrowth. Based on this broader definition of LULCC emissions it is clear that LULCC processes can be treated as emissions (i.e. E_L) or they could be included in the net land exchange term (i.e. N_L). Here we consider LULCC emissions explicitly in the E_L term, but this algebraic arrangement does not affect our error analysis. Factors contributing to errors in LULCC emission estimates can be separated into uncertainty in agricultural areas and rate of change in agricultural and forested areas, C density of natural and agricultural lands undergoing change, and uncertainty stemming from the definition of LULCC emissions (Gasser and Ciais, 2013; Pongratz et al., 2014). Emission estimates derived from these different approaches may differ by as much as 30% and over-all relative 2 σ errors on these individual approaches may be as high as 50% (Houghton et al., 2012). Therefore, even though CO_2 emissions associated with land-use change contribute a decreasingly smaller fraction of total CO_2 emissions, land use emission errors remain relatively high.

2.0 Methods: Identifying sources of error for terms in the global carbon budget

2.1 Errors in calculating the atmospheric growth rate

Documenting changes in CO_2 concentration based on atmospheric observations is not trivial, but fortunately the global observation network has expanded over the last 50 years allowing us to estimate changes in $\frac{\partial C}{\partial t}$ with greater confidence. Thus the error in estimating the atmospheric growth rate can be described as follows:

$$\frac{\widehat{dC}}{dt} = \frac{dC}{dt} \times (1 + \varepsilon_c) \qquad (2)$$

Where $\frac{\widehat{dC}}{dt}$ represents our estimate of the true annual growth rate of atmospheric CO_2 ($\frac{dC}{dt}$) and is calculated as the mean December and January (MDJ) concentrations of atmospheric CO_2 minus the MDJ values from the previous year (Thoning et al., 1989). Although atmospheric CO_2 is relatively well mixed on timescales greater than one year (Conway et al., 1994), there is considerable spatial and temporal error (ε_c) associated with estimating $\frac{\widehat{dC}}{dt}$ on annual timescales. For direct comparison with other terms in the global C budget, molar mixing ratios of atmospheric CO_2 are converted to a mass of petagrams (Pg= 10^{15}g) C using the conversion factor 2.124 PgC ppm^{-1} (Sarmiento et al., 2010).

2.1.1 Spatial Error Component of the Atmospheric CO_2 Growth Rate

Most of the error associated with calculating the changes in atmospheric CO_2 concentration from year to year is due to seasonal heterogeneities in the atmospheric mixing of atmospheric CO_2 and the spatial unevenness of the global observing network (http://www.esrl.noaa.gov/gmd/ccgg/). In fact, errors associated with the sampling network have been estimated to be about 1.2 PgC through cross-validation of individual sites using the entire global network (Masarie and Tans, 1995), which makes it challenging to substantiate annual growth rates that may only vary between 1 and 2 PgC yr^{-1} during early parts of the observational record (Ballantyne et al., 2012; Conway et al., 1994; Keeling et al., 1995).

To assess how much ε_C varies as a function of the non-random spatial distribution of the global observation network, we first subset the global network for 'background' sites in the marine boundary layer (MBL see Fig. 2) that are less affected by local anomalies in fossil fuel emissions and uptake (Masarie and Tans, 1995). To assess how biases in the MBL network may affect ε_C, bootstrap simulations were performed by simulating 100 alternative observation networks consisting of 40 sites that are resampled with replacement from sites located in the MBL. The only geographic constraint on resampling is that at least one site from the tropics, Arctic, Antarctic, North Pacific, and North Atlantic must be included in each simulated network. Since 1980, $\widehat{\frac{dC}{dt}}$ was estimated from all 100 simulated observation networks drawn from the MBL sites.

2.1.2 Temporal Error Component of the Atmospheric CO_2 Growth Rate

Because complete mixing of atmospheric CO_2 may take more than a year, errors in $\frac{dC}{dt}$ are not independent from year to year. In fact, errors in MDJ (ε_{MDJ}) values show considerable inter-annual positive autocorrelation, such that $\varepsilon_{MDJ\,(t)} = 0.244\ \varepsilon_{MDJ\,(t-1)} + 0.086\ \varepsilon_{MDJ\,(t-2)} + \varepsilon_{(t)}$, where $\varepsilon_{(t)}$ represents random error in the current year (Ballantyne et al., 2012). Because MDJ values that are biased high lead to $\frac{dC}{dt}$ estimates that are biased high in the previous year and biased low in the subsequent year, this leads to a negative autocorrelation, such that $\varepsilon_{C\,(t)} = -0.413\ \varepsilon_{C\,(t-1)} - 0.166\ \varepsilon_{C\,(t-2)} - 0.085\ \varepsilon_{C\,(t-3)} + \varepsilon_{(t)}$. Over the period prior to 1980, $\widehat{\frac{dC}{dt}}$ was calculated from atmospheric CO_2 observations at Mauna Loa and South Pole (MLOSPO) and ε_C was estimated from the ε_{MDJ} autocorrelated noise, as described above, normalized to a standard deviation of 0.24 ppm based on the period of observational overlap between MLOSPO and the MBL. Monthly mean MLOSPO values prior to 1974 were calculated from Scripps Institution of Oceanography Data (Keeling et al., 2005) and monthly mean MBL values were calculated from data collected by the National Oceanic and Atmospheric Administration's Earth System Research Laboratory (http://www.esrl.noaa.gov/).

2.2 Fossil Fuel Emissions

The process that currently accounts for the greatest flux of CO_2 to the atmosphere is the combustion of fossil fuels and cement production (i.e. E_F). Because fossil fuel emission estimates are derived from economically-constrained statistics of energy production and consumption, the relative errors in fossil fuel emission estimates are fairly small and typically between 5 and 10% (Andres et al., 2014). However, because fossil fuel emissions currently account for > 90% of total emissions, even relatively small errors can result in potentially large uncertainties in absolute C uptake calculated at the global scale (Francey et al., 2013; although see Raupach et al., 2013). Therefore identifying the sources of error in fossil fuel emission estimates $\widehat{E_F}$ is critical to constraining uncertainty in the global carbon budget:

$$\widehat{E_F} = E_F \times (1 + \varepsilon_F) \qquad (3)$$

where ε_F, the error factor in estimating fossil fuel emissions, has both a spatial and temporal component.

2.2.1 Spatial Error Component of Fossil Fuel Emissions

There are many sources of error in estimating fossil fuel emissions. In particular, fossil fuel emission inventories differ in their inclusion of CO_2 emissions from cement production and international transport, as well as their treatment of gas flaring (Andres et al., 2012). These subtle differences can equate to considerable discrepancies between different inventories (Fig. 3). Another significant source of error in global emission inventories is due to the different accounting practices of different nations. Although emission inventories are often based on standardized surveys of energy consumption, different institutions have different protocols for missing data and how units of energy are converted into CO_2 emissions (Andres et al. 2012). In some instances there may even be large discrepancies between the sum of provincial emission estimates and national emission estimates (Guan et al., 2012). All of these factors lead to uncertainties in emission estimates. While there is a general consensus that emission errors in developed nations are much lower than in developing nations, emissions are increasing at a faster rate simply because these nations are 'developing' rapidly.

For this analysis, countries were grouped into geographic regions as specified by the United Nations Statistics Division (http://unstats.un.org/unsd/methods/m49/m49regin.htm). Uncertainties for each country (see supplemental table 1; Andres et al. 2014) were used to create regional maximum error distributions for each emission inventory using a bootstrapping method, with the highest emitters within the region contributing the most to the error distributions. This effect was achieved by weighting the sampling probability ($P(s)$) by the relative contribution of each country's emissions (E_C) to the total emissions within that region (E_R): $P(s) = E_C/E_R$.

The bootstrapping method used 1000 iterations of the mean of sampled errors to produce a smoothed distribution for regional maximum errors. This method allows for bounded fluctuations in country-level annual errors that relate directly to regional errors. To constrain the temporal component of the emission errors (section 2.2.2), ten random samples were drawn from the corresponding error distribution for each country for each year from 1959–2010, producing ten random relative error time series for each country. These time series were used to produce the autocorrelated time series as described in section 2.2.2.

2.2.2 Temporal Error Component of Fossil Fuel Emissions

Fossil fuel accounting practices differ by individual nations, but these accounting practices often change over time as well. The errors in annual emission estimates are not independent from year to year. For instance, if an error is identified in annual emission calculations of a given country, then this error is corrected for the current year and all previous years emission estimates maybe retroactively corrected (Marland et al., 2009). Thus the errors in annual emission estimates are not necessarily independent over time. To account for this potential time-dependent error, we modified the conventional Monte-Carlo approach in which errors are randomly drawn for each year of the simulation to account for the known autocorrelation of errors in emission inventories. To distinguish this approach from the conventional Monte-Carlo approach, we refer to it as an 'el camino' method in which errors in the current year are dependent upon errors in previous years and thus the temporally correlated errors

follow a 'path' from year to year. This el camino approach allows for the incorporation of auto-correlated random noise into our fossil fuel emissions, such that:

$$\varepsilon_{F\,(t)} = 0.95 \times \varepsilon_{F\,(t-1)} + \varepsilon_{(t)}\,, \qquad (4)$$

where emission error factors for any given year $\varepsilon_{F\,(t)}$ are correlated with emission estimates from the previous year $\varepsilon_{F\,(t-1)}$ by an autoregressive coefficient of 0.95 with $\varepsilon_{(t)}$ as random error. Based on this formulation, the persistence of autocorrelation among errors in successive years is ~ 20 years. We note that our selection of ~20 years for the persistence of autocorrelation in emission error estimates is somewhat arbitrary; it assumes that errors are not corrected retroactively after 20 years. While it is conceivable that emission errors could be corrected going back even further in time, it has been shown that estimates tend to converge after a decade (Marland et al., 2009) therefore 2 decades is a fairly conservative estimate of the time-dependence of errors. For our analysis, we relied on three independent fossil fuel emission inventories (Fig. 3)- BP (previously known as British Petroleum), the Carbon Dioxide Information and Analysis Center (CDIAC), and the Emission Database for Global Atmospheric Research (EDGAR)- all of which included cement production as source of emissions.

2.3 Land Use Emissions

Among the variables in the global carbon budget (Eq 1), CO_2 emissions from land use and land change (E_L) are probably the most difficult to quantify and have the greatest error. This is because the net flux from E_L encompasses emissions resulting from the conversion of land from primary forest to agricultural production, in addition to C uptake associated with the abandonment of agricultural lands and the regrowth of secondary forest (Houghton, 1995). Many of these processes occur at local to regional scales; thus, there errors are difficult to propagate to the global scale. However, rates of deforestation and regrowth have changed over time and other environmental processes, such as N-deposition, climate variability and CO_2 fertilization may alter these rates (Jain et al., 2013). Here we consider the main factors contributing to the spatial and temporal components of E_L, such that:

$$\widehat{E_L} = E_L \times (1 + \varepsilon_L) \qquad . \qquad (5)$$

2.3.1 Spatial Error Component of Land Use Emissions

Land use emissions have remained fairly constant, or may have diminished, over the past 20 years, but patterns of deforestation associated with these emissions have clearly changed (Hansen et al., 2013; Houghton et al., 2012). Although recent estimates from Landsat imagery indicate that deforestation in Brazil have indeed gone down by approximately 1,300 km^2/yr in Brazil from 2000 to 2010 the last decade, this has almost been compensated by 1,000 km^2/yr increase in deforestation rates in Indonesia over the same period (Hansen et al. 2013), suggesting a regional shift in land use emissions but very little net change in land use change emissions over the last decade (Houghton et al. 2012). However, there are errors and assumptions associated with the conversion of forest area into CO_2 emission equivalents and the 2 σ relative error on emission estimates from land use change are thought to be on the order of 50% (Houghton Pers. Comm).

2.3.2 Temporal Error Component

Similar to errors in fossil fuel emission estimates, errors in CO_2 emissions from land use are also serially correlated. The benchmark method for estimating emissions from land use emissions is the bookkeeping approach developed by Houghton (1983) starts with global forestry statistics that are only released every five years (FAO, 2010). Thus net land-use emissions must be extrapolated for intervening years with no forestry statistics. Although this interpolation approach works fairly well when rates of deforestation and regrowth are not changing, this approach can lead to errors in estimating land-use emissions that once again are corrected retroactively. Therefore we apply a similar El Camino approach to simulating the auto-correlated errors in land use emissions by using the following relationship:

$$\varepsilon_{L\,(t)} = 0.05 \times \varepsilon_{L\,(t-1)} + \varepsilon_{(t)}\,, \qquad (6)$$

where the persistence of temporally correlated errors in land use emission is reduced to ~ 5 years. This time persistence value is arbitrary; however, it was selected based on the Food and Agricultural Organization's forestry statistics that are updated every five years. Therefore land-use emission estimates are predicted into the future four years and then corrected retroactively in the fifth year (Friedlingstein et al., 2010). Here we consider three independent estimates of E_L derived from three different approaches: 1.) The bookkeeping method based on forestry statistics (Houghton, 1995), 2.) a model derived estimate based on historical land use maps (Stocker et al., 2011), and 3.) a model derived estimate including historical land use as well as nitrogen cycling (Yang et al., 2010). Although more E_L estimates exist, we have selected three representative estimates of E_L covering a range of possible approaches for inclusion in our error analysis framework (Fig. 4).

2.4 Estimating net ocean and land uptake with uncertainty

2.4.1 Estimating net global C uptake

In order to estimate changes in the net global carbon uptake we focused on two diagnostic variables of the global carbon cycle. First we calculated net global carbon uptake by simply re-arranging equation 1 to solve for:

$$\Sigma N = \frac{\widehat{dC}}{dt} - \Sigma E \qquad , \qquad (7)$$

where we calculate net global uptake simply as the difference between the annual atmospheric growth rate and the sum of net emission fluxes to the atmosphere. Because we have defined the carbon mass balance with respect to the atmosphere a net loss from the atmosphere corresponds with negative ΣN as a result of increased carbon uptake by the biosphere. In order to calculate relative changes in global C uptake efficiency we also calculated the airborne fraction (*AF*), according to:

$$AF = \frac{\widehat{dC}}{dt} / \Sigma E \qquad , \qquad (8)$$

where an increase in *AF* would indicate an increase in the proportion of emissions remaining in the atmosphere and perhaps diminished C uptake efficiency by the biosphere.

To incorporate the error from different combinations of our fossil fuel emission simulations (E_{FX}) and our land-use emission simulations (E_{LX}), we devised an emission scenario matrix:

$$\Sigma E_{(FX,LX)} = \begin{bmatrix} E_{F1}+E_{L1} & E_{F1}+E_{L2} & E_{F1}+E_{L3} \\ E_{F2}+E_{L1} & E_{F2}+E_{L2} & E_{F2}+E_{L3} \\ E_{F3}+E_{L1} & E_{F3}+E_{L2} & E_{F3}+E_{L3} \end{bmatrix}, \qquad (9)$$

where $\Sigma E_{(FX,LX)}$ is a flexible framework that can accommodate any number of combinations of emission simulations. In our analysis we only consider three E_{FX} estimates and three E_{LX} estimates in our 3x3 matrix for a total of 9 different combinations of fossil fuel and land use emission combinations. Each combination consists of the sum of 500 fossil fuel emission simulations and 500 land use emission simulations with their associated spatial and temporal error spanning 52 years (ie. 1959 to 2010) for a grand total of 4500 x 52 simulations of $\Sigma E_{(FX,LX)}$ (Fig. 5). In order to calculate ΣN and AF we randomly drew from our $\frac{\partial C}{\partial t}$ simulations to perform 4500 calculations of ΣN and AF spanning from 1959 to 2010. We calculated ΣN and AF using two approaches, one, using the sum of all emissions as shown in the emission scenario matrix (eq. 9) and the other using just E_F simulations to assess how sensitive global C uptake is to these two different CO_2 emission scenarios.

2.4.2 Partitioning C uptake between the land and the ocean

In order to partition the global net C uptake flux between net land (i.e. N_L) and net ocean (i.e. N_O) uptake, we relied on ocean biogeochemical models that have been constrained by observations(Le Quéré et al., 2013) . In particular, these ocean biogeochemical models have been normalized to changes in atmospheric O_2/N_2 which provide an independent estimate of ocean C uptake mostly expressed on decadal time scales. We extended this logic, by using O_2/N_2 measurements to estimate the error in estimates of ocean C uptake in these ocean biogeochemical models:

$$\widehat{N_O} = N_O \times (1 + \varepsilon_O) \qquad (10)$$

where ε_O is the error in ocean C uptake and it is estimated from the atmospheric potential oxygen to be approximately 1.3 PgC yr^{-1} as the average 2σ error reported from Ishidoya et al. (2012) and (Manning and Keeling, 2006). Thus time invariant random normally distributed error (± ε_O) is added to each year of C uptake in each of the ocean biogeochemical models included in our analysis. For our analysis we considered ocean C uptake estimates from 5 independent ocean biogeochemical models- 1.) Nucleus for European Modeling of the Ocean (NEMO), 2.) Laboratory of Science and Climate of the Environment (LSCE), 3.) Community Climate System Model (CCSM-BEC), 4.) Norwegian Ocean Biogeochemical Model (MICOM-HAMOCC), 5.) Max Planck Institute (MPI-MET), that have all been included in the Global Carbon Projects 2013 assessment (Le Quéré et al., 2013). For each model, the random error term (ε_O) was added at each time step for a total of 900 realization of C uptake with error for each model for a grand total of 4500 realizations across models (Fig. 6). It should be noted that in order to calculate the ocean C uptake and its uncertainty from atmospheric measurements of O_2/N_2 fossil fuel emission estimates are required to constraint the 'atmospheric potential oxygen', thus the ε_O and the ε_F terms are not entirely independent. Nonetheless, O_2/N_2 measurements provide a measure of error which can be

applied to individual climate model simulations. These ocean C uptake realizations were then subtracted from our global uptake to infer net land uptake, according to:

$$\widehat{N_L} = \Sigma N - \widehat{N_O}\,. \qquad (11)$$

Thus yielding a distribution of 4500 simulations of ΣN, N_O, and N_L spanning the 1959 to 2010 observational period. From these simulations we estimate the significance of observed trends in ΣN, N_O, N_L, and *AF* over the last 5 decades as well as decadal changes in the mean value as well as the variance.

3 Results: sources of error and their impact on uptake uncertainty

3.1 Increasing precision and increasing variability in the atmospheric CO_2 growth rate

The error in calculating the annual atmospheric CO_2 growth rate has decreased considerably over the last 5 decades (Fig. 2). The mean overall 2σ error for $\frac{\widehat{dC}}{dt}$ was 0.71Pg C yr^{-1}, with a much higher 2σ error of 1.11 Pg C yr^{-1} from 1959 to 1980 and a much lower 2σ error from 1980 to the present of 0.36Pg C yr^{-1}. At the same time the variability in $\frac{\widehat{dC}}{dt}$ appears to have increased over the last 50 years. This is most clearly evident by inspecting decadal changes in the standard deviations of the annual mean values of $\frac{\widehat{dC}}{dt}$ (Table 1). During the 1960s $\frac{\widehat{dC}}{dt}$ values were much less variable (σ = 0.61 PgC yr^{-1}) than values of $\frac{\widehat{dC}}{dt}$ that peaked during the 1990s (σ = 1.40 PgC yr^{-1}) and have subsequently become slightly less variable since 2000 (σ = 0.82 PgC yr^{-1}). It is intriguing that variability in $\frac{\widehat{dC}}{dt}$ appears to be increasing while our precision in estimating $\frac{\widehat{dC}}{dt}$ has also increased. To test whether this increase in $\frac{\widehat{dC}}{dt}$ is simply due to adding sites to the global atmospheric CO_2 monitoring network, we examined the standard deviation in the atmospheric growth rate calculated from only the Mauna Loa and the South Pole monitoring sites. Although the over-all variance in $\frac{\widehat{dC}}{dt}$ was slightly reduced when calculated from only two sites, $\frac{\widehat{dC}}{dt}$ estimates show a similar increase in standard deviation from the 1960s (σ = 0.58 PgC yr^{-1}) through the 1990s (σ = 1.26 PgC yr^{-1}). Thus the apparent increase in carbon cycle variability over the last 50 years seems to be robust and not an artifact of the expanding global atmospheric CO_2 observation network.

In the early part of the observation record errors associated with estimating $\frac{\widehat{dC}}{dt}$ were one of the main contributors to uncertainty in calculating global C uptake; however, as the precision of $\frac{\widehat{dC}}{dt}$ estimates has increased, their contribution to global C uptake uncertainty has been reduced. In fact, in the 1960s errors in the atmospheric CO_2 growth rate accounted for roughly 40% of the uncertainty in global C uptake; in contrast, in the 2000s errors in the atmospheric CO_2 growth rate accounted for only about 10% of the uncertainty in global C uptake (Fig. 11). Thus errors in estimating the annual growth rate at the beginning of the period of observation (e.g. 1960s) made it difficult to determine if $\frac{\widehat{dC}}{dt}$ was in fact

statistically distinguishable from zero (Fig. 2); however, continued measurements have revealed that not only is $\frac{\widehat{dC}}{dt}$ positive but it is clearly accelerating as a result of increased emissions.

3.2 Increasing uncertainty in fossil fuel emission estimates

As of 2010, more than 90% of the total CO_2 emissions to the atmosphere were derived from fossil fuel combustion or cement production (Fig. 1), therefore slight errors in E_F can have significant impacts on C uptake estimates by the land and ocean. While fossil fuel emissions have increased by a factor of 3.6 over the past 50 years the absolute errors in fossil fuel emissions have increased by a factor 4.5 over the same period of time (Fig. 3), suggesting that fossil fuels account for an increasing proportion of the atmospheric CO_2 burden but that the precision of our E_F estimates is actually decreasing over time. This result is supported by the decadal statistics showing that the mean of the standard deviations has increased from the 1960s to present, while the standard deviation of the means has not changed appreciably (Table 1). This increase in E_F errors is due to the divergence in independent E_F inventories compounded by a greater contribution of emissions from emerging economies. Estimates of E_F from BP appear to be slightly higher than E_F estimates from CDIAC and EDGAR which are more similar to each other but slightly lower over the last 2 decades (Fig. 3). It is not quite clear what differences in accounting practices may cause these slight discrepancies between inventories, because they often rely on the same energy consumption statistics (Andres et al., 2012).

The other major source of error in fossil fuel emission estimates is from national reporting statistics that vary considerably based on the degree of development in energy infrastructure. While E_F errors are relatively low for North America, Europe, Australia, and parts of Asia, they are noticeably higher for some countries that emit a large portion of the global fossil fuel emissions, such as India, China and Russia. Lastly, the highest emission errors are for countries in South and Central America as well as some countries in Africa and the Middle East. These geographical regions with higher error are also located in regions with very few observations of atmospheric CO_2 making our ability to detect changes in net C uptake for these regions exceedingly difficult.

Lastly, errors in fossil fuel emissions are contributing a larger proportion to global C uptake uncertainty today than they were 50 years ago (Fig. 11). In the 1960s approximately 10% of the uncertainty in global C uptake could be attributed to errors in fossil fuel emission estimates, whereas approximately 30% of the global C uptake uncertainty is due fossil fuel emission errors since 2000. Furthermore, increasing trends in the errors of fossil fuel emissions are quickly becoming the dominant factor contributing to global C uptake uncertainty, with 38% of the total uncertainty due to emission errors in fossil fuels by the year 2010.

3.3 Land-Use emission errors remain high

Although emissions from land use land cover change (i.e. E_L) contribute much less to the total emissions to the atmosphere today than they did 5 decades ago, emission errors (i.e. ε_L) remain quite high (Fig. 4). Emissions from LULCC have remained fairly constant over the last 50 years, with an apparent decline over the last 20 years (Table 1). Because E_L has remained fairly constant while E_F has risen steadily over

the last 50 years, the fraction of total emissions comprised of E_L has declined to 10% since the year 2000, whereas E_L comprised almost 30% of the total emissions to the atmosphere during the 1960s.

Because errors in E_L are often reported as relative errors, they have gone down slightly in recent years as a function of decreasing emissions for independent estimates of E_L. However, these slight decreases in errors (ε_L) for independent land use emission estimates have been largely offset by the disagreement among independent estimates (Fig. 4). The combination of these factors has resulted in very little change in the overall error structure of E_L over the last 50 years (Table 1). Because E_L and ε_L have remained fairly constant over the last 5 decades the proportion of error contributed to global uncertainty in C uptake has remained at approximately 0.4 (Fig. 11).

3.4 Changes in net global C uptake and the airborne fraction

A clear and significant acceleration in net global C uptake has been observed from 1959 to 2010, with net rates of annual ΣN nearly doubling from 2.2 ± 1.8 PgC yr^{-1} in 1959 to 4.3 ± 1.6 PgC yr^{-1} in 2010 (± 2σ). This acceleration in ΣN corresponds to a 0.5 PgC $decade^{-1}$ increase in the amount of C taken up by Earth over the past 50 years (Fig. 7). Furthermore this increasing trend in net global C uptake, as evidenced by progressively more negative ΣN values appears to be insensitive to whether land-use emissions are included in our global C budget (Figs. 8A and 8B). For both emission scenarios with and without land use emissions ΣN trends were all negative. In fact, when E_L emissions are removed from our calculations of ΣN we see that the trend in ΣN actually increases from -0.05 PgC yr^{-1} to -0.06 PgC yr^{-1} (see median values in Figs. 8A and 8B). Although a clear and significant increase in ΣN is evident over the last 50 years, there is considerable decadal variability as well. We see that ΣN increased by ~30% from the 1960s to the 1970s, but only a ~5% increase in ΣN was observed from the 1990s to the 2000s (Table 1). This suggests that the increase in global C uptake has not been a steady increase, but can be characterized by periods of rapid acceleration and periods of slow or no acceleration (Table 1). The decadal means of the standard deviations of ΣN have steadily gone down over the last 50 years, indicating that our ability to detect changes in global C uptake has improved (Table 1). However, this increased detection ability of ΣN over time has been somewhat undermined by the recent uptick in global C uptake uncertainty over the last 10 years, due to increasing errors in fossil fuel emission estimates (Fig. 11). In contrast, the decadal standard deviation of the mean values of ΣN have increased over the last 50 years, indicating an increase in the observed variability of global C uptake that appears to have peaked at 1.37 PgC yr^{-1} during the 1990s (Table 1).

The airborne fraction of atmospheric CO_2 has only increased slightly over the last 5 decades, but this increase is not significant (Fig. 7). Furthermore, the airborne fraction appears to be highly sensitive to whether land-use emissions are included in our emission scenario. For instance, mostly positive trends were observed in AF when both land-use and fossil-fuels were included in our emission scenario, indicating a possible increase in AF and a possible decrease in relative global C uptake efficiency (Fig. 8C). However, if we consider the fossil fuel only scenario, we see that the sign of AF trends become almost exclusively negative indicating a possible increase in relative global C uptake efficiency (Fig. 8D). Although no significant trend in AF was observed within the bounds of uncertainty of our analysis, a considerable decrease in annual AF variance was observed over the 50 year record of observations (Fig.

7). The decadal mean of the standard deviations has gone down from 0.16 in the 1960s to 0.03 in the 2000s; such a decrease indicates that our ability to detect changes in *AF* has increased by a factor of four. Similar to our *ΣN* statistics, the standard deviation of the decadal means in *AF* has climbed steadily until the 1990s suggesting that variability in the global C cycle peaked in the 1990s and has remained strong.

3.5 Changes in the partitioning of C uptake between the ocean and land

Both land and ocean C uptake have increased over the last 50 years; however, variability in this C uptake is quite different for these two components of the global C cycle (Fig. 9). The median value of our 4500 simulated N_O trends was -0.031 PgC yr^{-2} and 97% of these simulated trends were negative (4378/4500), providing strong evidence that ocean C uptake as simulated by ocean biogeochemical models has increased over the last 50 years. Similarly, the median value for our inferred trends of N_L was -0.024 PgC yr^{-2}, with 93% of our simulations showing negative N_L trends (4185/4500). Therefore given the full range of errors considered in our analysis of atmospheric CO_2 observations and emission estimates, we can say with an extremely high level of confidence that ocean C uptake has increased steadily and with a high level of confidence that land C uptake has increased but with greater variability over the last 50 years.

Although empirical evidence clearly shows that rates of ocean and land C uptake have increased, decadal variability of N_O and N_L show quite different patterns over the last 50 years. Rates of N_O have increased from 1.11 ± 1.31 PgC yr^{-1} during the 1960s to 2.21 ± 1.39 PgC yr^{-1} during the 2000s (Table 1). Even though N_O rates have increased in every decade over which we have observationally constrained estimates, the percentage of increase in N_O has gone down from a 29% increase from the 1960s to 1970s to only an 8% increase from the 1990s to 2000s. Over the past five decades, the mean of the standard deviations in N_O has remained fairly constant, but increased slightly since 2000 possibly due to a divergence in model predictions (Fig. 6). An alternative perspective is provided by the coefficient of variation of N_O which has gone down steadily over the last 50 years from ~ 1.5 to ~0.6, suggesting that our ability to detect changes in N_O has increased considerably (Fig. 10).

Much more variability in net land C uptake was observed from annual to decadal scales over the last 50 years. Rates of N_L have increased from 1.39 ± 1.56 PgC yr^{-1} during the 1960s to 2.46 ± 1.43 PgC yr^{-1} during the 2000s (Table 1); however considerable variability in N_L was also observed (Fig. 8). For instance, in 1987 (N_L = 0.31 ± 1.40 PgC yr^{-1}) and 1998 (N_L = 0.82 ± 1.58 PgC yr^{-1}) a net release of CO_2 from the terrestrial biosphere to the atmosphere is inferred. Decadal variability in N_L also appears to be increasing as evidenced by the increase in the standard deviation of the annual mean N_L values from 0.56 PgC yr^{-1} in the 1960s to 1.06 PgC yr^{-1} in the 2000s, with a peak in variance occurring during the decade of the 1990s (Table 1). Although net land C uptake appears to have become increasingly variable on decadal scales over the last 5 decades, our ability to detect changes in land C uptake and its inter-annual variability has improved. The mean of standard deviations of N_L has decreased from 1.56 PgC yr^{-1} in the 1960s to 1.43 PgC yr^{-1} in the 2000s, suggesting that our annual estimates of N_L are becoming more constrained over time (Table 1). This is also reflected in a slight decrease in the coefficient of variation of N_L from ~ 1.0 in the 1960s to ~0.5 in the 2000s, albeit with much greater inter-annual differences (Fig. 10). Incidentally, both years that showed a net release of CO_2 from the terrestrial biosphere to the

atmosphere also showed relatively high coefficients of variation as the mean of N_L approached zero in our simulations.

4.0 Discussion

4.1 Atmospheric Growth Rate

The stabilization of atmospheric CO_2 concentrations is one of the greatest challenges to humanity; however, it is worth pointing out that in order to stabilize atmospheric CO_2 concentrations we must first stabilize the atmospheric CO_2 growth rate. Unfortunately, there is no indication that the atmospheric CO_2 growth rate is stabilizing; in fact, it has accelerated over the last 50 years (0.05 PgC yr^{-2}; P-value= 7.5 x 10^{-7}), such that every decade the growth rate has increased by half a petagram of C per year. Although the atmospheric CO_2 growth rate has clearly accelerated it has not accelerated smoothly on decadal time scales. For instance, during the 1980s the growth rate of atmospheric CO_2 accelerated only slightly (0.04 PgC yr^{-2}), compared to the 1990s when the atmospheric growth rate accelerated rapidly (0.17 PgC yr^{-2}). While it has been suggested that these decadal changes in the growth rate of atmospheric CO_2 are perhaps due to emission errors (Francey et al., 2013), our analysis suggests that this decadal variability is more likely due to variability in terrestrial C uptake consistent with previous analyses (Bousquet et al., 2000; Sarmiento et al., 2010).

Our ability to detect changes in atmospheric CO_2 has increased considerably as additional sites have been added to the global monitoring network. The error in calculating $\frac{\widehat{dC}}{dt}$ has decreased by a factor 4 from a mean value of 1.2 PgC during the 1960s to 0.3 PgC during the 2000s. Even though the annual mean of $\frac{\widehat{dC}}{dt}$ has increased rapidly over the last 50 years the standard deviation about this annual mean has decreased even faster, as evidenced by the annual coefficient of variation in $\frac{\widehat{dC}}{dt}$ that has gone down by a factor 10 from 0.37 in the 1960s to 0.04 in the 2000s. This increase in signal to noise ratio of $\frac{\widehat{dC}}{dt}$ once again clearly illustrates our increased ability to detect annual changes in atmospheric CO_2 at the global scale. However, estimating global changes in $\frac{\widehat{dC}}{dt}$ from observations at an array of background sites is relatively easy compared to estimating regional changes in $\frac{\widehat{dC}}{dt}$ from continental sites even when an extensive network of frequent observations are available. For instance, Gourdji et al. (2012) found a 0.8 PgC yr^{-1} difference between two atmospheric inversion estimates of the C budget for N. America depending on two different sets of boundary layer mixing ratios of CO_2, which is close to our 2 σ uncertainty of 1.2 PgC yr^{-1} for global C uptake for the year 2010. Therefore verifying potential changes in net CO_2 fluxes at the regional to continental scale remains a challenge and hopefully advances in satellite measurements, including the recently launched orbiting carbon observatory, in combination with surface measurements (Miller et al., 2014).

4.2 Fossil Fuel Emissions

At the inception of continuous atmospheric CO_2 measurements in 1959, fossil fuel emissions constituted approximately 75% of the total emissions to the atmosphere; however, as fossil fuel emissions have

increased so has their relative contribution to the atmospheric burden of which fossil fuels now contribute > 90% (Table1). As fossil fuel emissions have become the dominant driver of increasing atmospheric CO_2 concentrations, absolute errors from fossil fuel emissions have also increased steadily thus causing a slight increase in uncertainty of global C uptake in recent years (Fig. 11).

The greatest source of error in fossil fuel emission estimates is derived from national energy consumption statistics that can be as high as 20% of total emissions for some nations (Fig. 3) and may be even higher in some years due to the temporally correlated errors in emission estimates (Marland et al., 2009). Although the large errors in emission estimates have long been suspected, they have only recently been identified and quantified. For instance, by comparing provincial and national fossil fuel emission estimates in 2010, Guan et al. (2012) revealed a 1.4 Pg discrepancy between national emission estimates that appear to be biased low and provincial emission estimates that appear to be biased high (Guan et al., 2012). This difference in fossil fuel emission estimates from China alone amounts to approximately 15% of the total global emissions for 2010. Similar analyses have not yet been conducted for other large emitting nations, but discrepancies probably exist in the reporting practices of many nations. If the absolute fossil fuel emission errors continue to grow, they will start to undermine our ability to estimate C uptake by the biosphere, especially at the regional scale (Francey et al., 2013). It is also noteworthy that some emission estimate errors may be simply accounting mistakes that do not require retroactively correcting previous estimates, and other errors may be improvements to protocols that may require retroactively correcting previous estimates, so our time-dependent error approach is more appropriate for the latter revisions to accounting protocols.

4.3 Land Use Emissions

Total emissions from land use change have gone down slightly over the last 2 decades and now rival the errors in fossil fuel emissions. As of 2010 the 2 σ error of F_F was approximately ± 0.59 PgC yr^{-1}, whereas the total E_L was 0.76 ± 0.98 PgC yr^{-1} , clearly illustrating that E_L fluxes are contributing a smaller proportion to the overall atmospheric CO_2 burden and that errors in estimating the E_L term remain quite large. This suggests that efforts to reduce the atmospheric CO_2 growth rate or its concentration should focus primarily on reducing fossil fuel emissions and secondarily on changes in land use practices. Policies designed to reduce emissions from deforestation and forest degradation (so-called REDD programs) have been widely promoted; however, it is clear that fossil fuel emissions currently dwarf land use emissions. Therefore current policies aimed at Reducing Emissions from Deforestation and Degradation (REDD) maybe misguided and their effectiveness maybe difficult to quantify (Matthews et al., 2014). Although C uptake is one of the most important ecosystem services currently provided by the terrestrial biosphere at the global scale, it is certainly not the only ecosystem service provided by the terrestrial biosphere.

Our analysis indicates the need to reduce the uncertainty in what constitutes land use emissions and how their errors are calculated. Although LULCC emission estimates from bookkeeping approaches and process model approaches are fairly comparable, discrepancies among these approaches may in fact be due to differences in the operational definition of what constitutes LULCC emissions (Houghton, 2013; Pongratz et al., 2014). In fact, LULCC emission estimates differ by as much as 30% suggesting that 1/3 of

the uncertainty in LULCC emissions is simply due to differences in terminology leading to differing treatments of deforestation and regrowth. Further, the errors on LULCC emission estimates are poorly constrained with model simulations often not reporting estimate errors (Le Quéré et al., 2013) or bookkeeping methods often reporting relative errors. Land use emissions have gone down slightly from ~ 1.5 PgC yr^{-1} to 1.0 PgC yr^{-1} over the last 5 decades, so based on a relative 2 σ emission error of 50% one would conclude that absolute errors have also gone down from 0.75 PgC yr^{-1} to 0.50 PgC yr^{-1}. However, based on the discrepancies among approaches it is clear that absolute error have probably remained fairly constant over the last 5 decades (Fig. 4). Discrepancies among the different operational definitions of land use emissions and their impacts on the global C budget have been identified previously and methodological frameworks have been proposed for reconciling these different operational definitions and their estimates (Gasser and Ciais, 2013).

4.4 Changes in Land and Ocean C uptake and their implications

It is clear from our analysis that both the land and ocean biosphere continue to provide a tremendous climatic benefit by absorbing more than 50% of the total CO_2 that has been emitted to the atmosphere over the last 50 years. According to our estimates, net global C uptake (i.e. ΣN) has nearly doubled over the last 50 years. While some evidence suggests that terrestrial C uptake may be waning in the Southern Hemisphere tropics (Zhao and Running, 2010) due to water stress and that the C uptake in the Southern Ocean might be reduced by increased surface winds (Le Quéré et al., 2007), our analysis indicates that these potential regional declines in both terrestrial and ocean C uptake are more than compensated by increased C uptake elsewhere in the biosphere. At the same time our ability to detect changes in ΣN has increased (Fig. 7), as evidenced by the decrease of the mean of the standard deviations by decade (Table 1). This reduced uncertainty in our ability to quantify ΣN is mainly due to the reduced error in our estimates of the atmospheric growth rate due to the addition of sites to the global observing network (Fig. 11).

Another important diagnostic of how the global C cycle may be responding to concomitant changes in atmospheric CO_2 and climate is the airborne fraction (i.e. *AF*), which provides a useful estimate of possible changes in C uptake efficiency by the biosphere. A possible increase in *AF* over the last 5 decades has been identified (Canadell et al., 2007) and attributed to a decrease in the efficiency with which C is being removed from the atmosphere by land and ocean sinks (Le Quéré et al., 2009). Our analysis suggests that there is considerable uncertainty with respect to possible trends in *AF*, where the sign of the *AF* trend is slightly positive when including both fossil fuels and land use in our emission scenarios but the trend becomes negative if we do not consider land use in our emission scenarios. This result is consistent with Knorr (2009) who found that any apparent trend in *AF* was not statistically distinguishable from zero, suggesting that there is too much uncertainty in the *AF* calculation to determine whether a trend is evident over the last 5 decades. It should also be noted that previous analyses were only able to identify a possible trend in *AF* after removing interannual variability in the atmospheric growth rate due to volcanic activity and El Nino, making interpretation of any changes in th unitless relative *AF* even more difficult. Furthermore, it has been demonstrated from model simulations that changes in *AF* are more likely to be sensitive to rapid changes in fossil fuel emissions than C uptake efficiency (Gloor et al., 2010). However, it is important to note that the error associated with

calculating *AF* appears to have gone down, which may make *AF* a more sensitive diagnostic of C cycle changes in the future.

The net exchange of carbon between the terrestrial biosphere and the atmosphere is challenging to estimate directly and can only be inferred; however, more tightly constrained estimates of the atmospheric CO_2 growth rate have greatly reduced the error associated with the inferred residual C sink. As net global C uptake uncertainty has diminished (Fig. 11), so has uncertainty in our calculation of net Land C uptake (i.e. N_L). Indeed our estimates, of N_L show an over-all decrease in the mean of the standard deviation over the last 5 decades, which indicates that once again our ability to detect changes in N_L has improved in recent years (Table 1). While our estimates of changes in terrestrial C uptake are largely inferred as a byproduct ocean biogeochemical models, more recently derived independent observationally based estimates of ocean C uptake (Khatiwala et al., 2009; Majkut et al., 2014) will allow for more observational constraints on the largely inferred residual land C sink.

It is clearly evident that net land C uptake has increased over the last 50 years (Fig. 9). Independent analyses from observations and models corroborate our findings that the absolute value of N_L has increased over the last 5 decades. A synthesis of data on C budgets of the world's forests concluded that terrestrial C uptake has remained strong and fairly constant from 1990 through the 2000s (Pan et al., 2011). In their synthesis Pan et al. (2011) conclude that N_L was 2.5 ± 0.4 PgC yr^{-1} during the 1990s and only decreased slightly to 2.3 ± 0.5 PgC yr^{-1} from 2000 to 2007. These estimates are fairly close to our estimates, although our estimates indicate a slight increase in N_L from the 1990s (2.35 ± 1.5 PgC yr^{-1}) to the 2000s (2.46 ± 1.4 PgC yr^{-1}), but with greater uncertainty (Table 1). It should be noted that there is considerable decadal variability in N_L and that the conclusions from Pan et al. (2011) might have been completely different had they compared the 1970s to the 1980s over which time the amount of C uptake by the terrestrial biosphere actually decreased as evidenced by an increase in N_L (Table 1.). Increases in terrestrial C uptake are also evident in estimates from dynamic vegetation models and atmospheric inversion studies, which both show terrestrial C uptake increasing from 1980 and peaking in 2011 (Poulter et al., 2014).

While net terrestrial C uptake has increased over the last 5 decades, the variability in net land C uptake appears to have increased as well. In fact, the standard deviation of the means in decadal C uptake by the terrestrial biosphere increased by almost a factor 3 from the 1960s through the 1990s and since 2000 the variability in net terrestrial C uptake has gone down slightly (Table 1). Although several well documented stochastic events occurred during the latter half of the observational record, including two strong El Nino events in 1987 and 1997 as well as the eruption of Mt. Pinatubo in 1991, there remains an apparent increase in variability of net C uptake by the terrestrial biosphere. More recently semi-arid ecosystems have been identified as regions of increased photosynthetic activity and potentially enhanced C uptake (Donohue et al., 2013; Poulter et al., 2014) ; however, it should be noted that these ecosystems are often the most vulnerable to carbon loss due to disturbance (Reichstein et al., 2013) and thus increased C uptake during favorable climate conditions may be followed by increased C loss during extreme climate events ultimately leading to the increased variance in net terrestrial C uptake observe in our analysis. It is also worth pointing out that in some instances when multiple disturbances of sufficient magnitude force the carbon system in the same direction their effect can be detected in the

atmosphere. For instance, one of the most severe El Nino events occurred in 1997 and this event was associated with widespread tropical drought that was thought to reduce photosynthesis at a global scale (Nemani et al., 2003). However, the impact of this random climatic event was greatly exacerbated by land use practices in South East Asia that promoted the draining of peatlands, which subsequently burned during the El Nino event (Ballhorn et al., 2009). Thus providing evidence of how compound disturbances to the terrestrial C cycle can actually be detected in the atmosphere. It remains to be seen whether this variability is simply the slow resilience of the biosphere to global perturbations, or if this increased variance indicates a potential regime shift in the terrestrial C cycle (Reichstein et al., 2013).

Based on our error analysis across a range of ocean biogeochemical models there is no clear indication that ocean C uptake has diminished over the last 50 years. Although ocean C uptake appears to have accelerated steadily by 0.2 and 0.3 PgC yr^{-1} $decade^{-1}$ from the 1960s to the 1990s, ocean C uptake may have decreased slightly to 0.14 PgC yr^{-1} over the last decade. However, at the same time the mean of the annual standard deviations also increased over the last decade suggesting less agreement among ocean models making it more difficult to detect the possible early stages of ocean CO_2 saturation. Much of the discussion regarding possible CO_2 saturation of the oceans has focused on the Southern Ocean because it contributes such a large portion (0.4 Pg C yr^{-1}) to the recent net global annual ocean C uptake of ~ 2.0 Pg C yr^{-1} (Le Quéré et al., 2007; Lovenduski et al., 2007). Unfortunately, this is a region of the Earth for which atmosphere CO_2 measurements and oceanic pCO2 measurements are fairly scarce. In fact, estimates between ocean biogeochemical models (0.42 ± 0.07 Pg C yr^{-1}) and observational constraints (0.27 ± 0.13 Pg C yr^{-1}) for the Southern Ocean are not even in statistical agreement (Lenton et al., 2013), suggesting that possible CO_2 saturation of the Southern Ocean would be extremely difficult to detect if it were in fact occurring given the current configuration of the global C observation network. It should also be noted that factors influencing the kinetics of air-sea gas exchange and how they are incorporated into these ocean biogeochemical models may have a large impact on global estimates of $N_{O.}$ For instance, the gas transfer velocity term used in calculating N_O incorporates a solubility function and wind speed function neither of which are linear functions (Wanninkhof et al., 2013). Although these functions have been optimized based on empirical studies, it is not known how much regional variability there is in these functions and whether it is valid to apply a universal air-sea gas exchange parameterization to all ocean basins.

Although the climate benefit conferred by increased land and ocean C uptake is irrefutable, this climate benefit may come at some expense of the biosphere to provide other vital ecosystem services. The greatest and most easily quantified impact of increased C uptake has been on the oceans through decreases in pH. It has been estimated that pH of the ocean has decreased by 0.1 over the last 50 years which is equivalent to a 20% increase in hydrogen ion concentration (Doney et al., 2009) . This increase in ocean acidity is particularly harmful for calcareous organisms, especially those with shells formed from aragonite, such as corals that form the base of many tropical marine ecoystems and pteropods that form the base of many pelagic marine ecosystems (Doney et al., 2009). Although some studies suggest that increased dissolved inorganic carbon in the water column may stimulate the biologic pump and thus primary productivity in the ocean (Riebesell et al., 2007), the direct impacts of acidification on

calcareous organisms and the indirect impacts of increasing sea surface temperatures are thought to have a net negative effect on ocean productivity (Doney et al., 2009).

In contrast, the direct impacts of rising CO_2 on the terrestrial biosphere may be both positive and negative. For instance, the fertilizing effect of increasing atmospheric CO_2 on photosynthesis in terrestrial plants is well documented (Ainsworth and Long, 2005), leading to potential increases in water-use efficiency as terrestrial plants become more frugal with water losses through transpiration (Keenan et al., 2013). Although the detrimental effects of increasing atmospheric CO_2 on the terrestrial biosphere are not as obvious, they may be just as insidious. For instance, increasing atmospheric CO_2 has been implicated in accelerated weathering of bedrock (Andrews and Schlesinger, 2001), which can release both harmful and beneficial elements from Earth's lithosphere into terrestrial ecosystems (Mast et al., 2011). It has also been suggested that CO_2 fertilization may differentially affect the growth of plant species, with faster growth in epiphytes such as lianas leading to tree mortality (Phillips et al., 2002). While detrimental impacts of increased atmospheric CO_2 on terrestrial ecosystems are more challenging to identify, because CO_2 is well-mixed on annual timescales there is no ecosystem on Earth that has not been impacted by its increasing concentration and more detrimental impacts will undoubtedly be identified in the future.

5.0 Conclusions:

As scientists it is no longer sufficient to simply arrive at an estimate; we must bound our estimates with some level of confidence. This is particularly important when investigating something as important as the global C cycle and the climate sensitivity of carbon sinks that continue to take up atmospheric CO_2. Because the topic of carbon-climate feedbacks is critical for both political and social decisions at the global scale, we must provide the public with the best estimates of important terms in the global carbon budget and their respective uncertainties. The uncertainty that arises from measurement, analytical and estimate errors is important because it provides scientists and policy makers alike a metric by which to weight the information provided when it is incorporated into their decision making framework. For instance, the effectiveness of policies targeted at fossil fuel emissions with their relatively high rates and low errors may easier to verify than the effectiveness of policies targeted at land use emissions that are fraught with uncertainty. In fact, errors associated with fossil fuel emissions are now comparable to total emissions from changes in LULCC (Table 1). Here we have created a framework by which estimate errors can be explicitly incorporated into the global C budget, allowing for the calculation of uncertainty in global C uptake. We have identified some major sources of error and their important spatial and temporal components; however, we acknowledge that latent sources of error do exist and thus can be incorporated into the flexible framework that we have created. Despite the many sources of error that we have identified in estimating terms in the global C budget, we conclude with an extremely high level of confidence that ocean C uptake has increased over the past 50 years and with a high level of confidence that land C uptake has also increased.

Acknowledgments:

788 This research was supported by grants from NSF and NRC to AP Ballantyne. This work would not have
789 been possible without the continuous atmospheric sampling efforts of dozens of volunteer scientists
790 from around the world and careful measurements by researchers at NOAA ESRL. We would also like to
791 thank Gregg Marland and students in the emerging topics in ecosystem science seminar at the
792 University of Montana for positive feedback.

793

794

795

References

Ainsworth, E. A., and S. P. Long, 2005, What have we learned from 15 years of free-air CO2 enrichment (FACE)? A meta-analytic review of the responses of photosynthesis, canopy properties and plant production to rising CO2: New Phytologist, v. 165, p. 351-372.

Andres, R., T. Boden, and D. Higdon, 2014, A new evaluation of the uncertainty associated with CDIAC estimates of fossil fuel carbon dioxide emission: Tellus, v. 66.

Andres, R. J., T. A. Boden, F.-M. Bréon, P. Ciais, S. Davis, D. Erickson, J. S. Gregg, A. Jacobson, G. Marland, and J. Miller, 2012, A synthesis of carbon dioxide emissions from fossil-fuel combustion: Biogeosciences Discussions, v. 9.

Andrews, J. A., and W. H. Schlesinger, 2001, Soil CO2 dynamics, acidification, and chemical weathering in a temperate forest with experimental CO2 enrichment: Global Biogeochemical Cycles, v. 15, p. 149-162.

Bakker, D., S. Hankin, A. Olsen, B. Pfeil, K. Smith, S. Alin, C. Cosca, B. Hales, S. Harasawa, and A. Kozyr, 2014, An update to the Surface Ocean CO2 Atlas (SOCAT version 2): Earth.

Ballantyne, A., C. Alden, J. Miller, P. Tans, and J. White, 2012, Increase in observed net carbon dioxide uptake by land and oceans during the past 50 years: Nature, v. 488, p. 70-72.

Ballhorn, U., F. Siegert, M. Mason, and S. Limin, 2009, Derivation of burn scar depths and estimation of carbon emissions with LIDAR in Indonesian peatlands: Proceedings of the National Academy of Sciences, v. 106, p. 21213-21218.

Boden, T. A., G. Marland, and R. J. Andres, 2009, Global, regional, and national fossil-fuel CO2 emissions: Carbon Dioxide Information Analysis Center, Oak Ridge National Laboratory, US Department of Energy, Oak Ridge, Tenn., USA doi, v. 10.

Bousquet, P., P. Peylin, P. Ciais, C. Le Quéré, P. Friedlingstein, and P. P. Tans, 2000, Regional changes in carbon dioxide fluxes of land and oceans since 1980: Science, v. 290, p. 1342-1346.

Canadell, J. G., P. Ciais, K. Gurney, C. Le Quéré, S. Piao, M. R. Raupach, and C. L. Sabine, 2011, An international effort to quantify regional carbon fluxes: Eos, Transactions American Geophysical Union, v. 92, p. 81-82.

Canadell, J. G., C. Le Quéré, M. R. Raupach, C. B. Field, E. T. Buitenhuis, P. Ciais, T. J. Conway, N. P. Gillett, R. Houghton, and G. Marland, 2007, Contributions to accelerating atmospheric CO2 growth from economic activity, carbon intensity, and efficiency of natural sinks: Proceedings of the national academy of sciences, v. 104, p. 18866-18870.

Conway, T. J., P. P. Tans, L. S. Waterman, K. W. Thoning, D. R. Kitzis, K. A. Masarie, and N. Zhang, 1994, Evidence for interannual variability of the carbon cycle from the National Oceanic and Atmospheric Administration/Climate Monitoring and Diagnostics Laboratory global air sampling network: Journal of Geophysical Research: Atmospheres (1984–2012), v. 99, p. 22831-22855.

Dai, M., Z. Cao, X. Guo, W. Zhai, Z. Liu, Z. Yin, Y. Xu, J. Gan, J. Hu, and C. Du, 2013, Why are some marginal seas sources of atmospheric CO2?: Geophysical Research Letters, v. 40, p. 2154-2158.

DeFries, R., C. Field, I. Fung, G. Collatz, and L. Bounoua, 1999, Combining satellite data and biogeochemical models to estimate global effects of human-induced land cover change on carbon emissions and primary productivity: Global Biogeochemical Cycles, v. 13, p. 803-815.

Doney, S. C., V. J. Fabry, R. A. Feely, and J. A. Kleypas, 2009, Ocean acidification: the other CO2 problem: Marine Science, v. 1.

Donohue, R. J., M. L. Roderick, T. R. McVicar, and G. D. Farquhar, 2013, Impact of CO2 fertilization on maximum foliage cover across the globe's warm, arid environments: Geophysical Research Letters, v. 40, p. 3031-3035.

FAO, 2010, Global Forest Resources Assessment 2010, FAO Forestry paper, Rome.

Francey, R. J., C. M. Trudinger, M. van der Schoot, R. M. Law, P. B. Krummel, R. L. Langenfelds, L. P. Steele, C. E. Allison, A. R. Stavert, and R. J. Andres, 2013, Atmospheric verification of anthropogenic CO2 emission trends: Nature climate change, v. 3, p. 520-524.

Friedlingstein, P., R. Houghton, G. Marland, J. Hackler, T. A. Boden, T. Conway, J. Canadell, M. Raupach, P. Ciais, and C. Le Quere, 2010, Update on CO2 emissions: Nature Geoscience, v. 3, p. 811-812.

Gasser, T., and P. Ciais, 2013, A theoretical framework for the net land-to-atmosphere CO 2 flux and its implications in the definition of" emissions from land-use change": Earth System Dynamics Discussions, v. 4, p. 179-217.

Gloor, M., J. Sarmiento, and N. Gruber, 2010, What can be learned about carbon cycle climate feedbacks from the CO 2 airborne fraction?: Atmospheric Chemistry and Physics, v. 10, p. 7739-7751.

Gourdji, S. M., K. Mueller, V. Yadav, D. Huntzinger, A. Andrews, M. Trudeau, G. Petron, T. Nehrkorn, J. Eluszkiewicz, and J. Henderson, 2012, North American CO 2 exchange: inter-comparison of modeled estimates with results from a fine-scale atmospheric inversion: Biogeosciences, v. 9.

Guan, D., Z. Liu, Y. Geng, S. Lindner, and K. Hubacek, 2012, The gigatonne gap in China/'s carbon dioxide inventories: Nature Climate Change, v. 2, p. 672-675.

Hansen, M., P. Potapov, R. Moore, M. Hancher, S. Turubanova, A. Tyukavina, D. Thau, S. Stehman, S. Goetz, and T. Loveland, 2013, High-resolution global maps of 21st-century forest cover change: science, v. 342, p. 850-853.

Houghton, R., J. Hobbie, J. M. Melillo, B. Moore, B. Peterson, G. Shaver, and G. Woodwell, 1983, Changes in the Carbon Content of Terrestrial Biota and Soils between 1860 and 1980: A Net Release of CO" 2 to the Atmosphere: Ecological monographs, v. 53, p. 235-262.

Houghton, R., J. House, J. Pongratz, G. van der Werf, R. DeFries, M. Hansen, C. Le Quéré, and N. Ramankutty, 2012, Carbon emissions from land use and land-cover change: Biogeosciences, v. 9.

Houghton, R. A., 1995, Land-use change and the carbon cycle: Global change biology, v. 1, p. 275-287.

Houghton, R. A., 2013, Keeping management effects separate from environmental effects in terrestrial carbon accounting: Global change biology, v. 19, p. 2609-2612.

Ishidoya, S., S. Aoki, D. Goto, T. Nakazawa, S. Taguchi, and P. K. Patra, 2012, Time and space variations of the O2/N2 ratio in the troposphere over Japan and estimation of the global CO2 budget for the period 2000-2010: Tellus B, v. 64.

Jain, A. K., P. Meiyappan, Y. Song, and J. I. House, 2013, CO2 emissions from land-use change affected more by nitrogen cycle, than by the choice of land-cover data: Global change biology, v. 19, p. 2893-2906.

Keeling, C., T. Whorf, M. Wahlen, and J. v. d. Plicht, 1995, Interannual extremes in the rate of rise of atmospheric carbon dioxide since 1980: Nature, v. 375, p. 666-670.

Keeling, C. D., 1960, The concentration and isotopic abundances of carbon dioxide in the atmosphere: Tellus, v. 12, p. 200-203.

Keeling, C. D., S. C. Piper, R. B. Bacastow, M. Wahlen, T. P. Whorf, M. Heimann, and H. A. Meijer, 2005, Atmospheric CO2 and 13CO2 exchange with the terrestrial biosphere and oceans from 1978 to 2000: observations and carbon cycle implications, A history of atmospheric CO2 and its effects on plants, animals, and ecosystems, Springer, p. 83-113.

Keeling, C. D., S. C. Piper, T. P. Whorf, and R. F. Keeling, 2011, Evolution of natural and anthropogenic fluxes of atmospheric CO2 from 1957 to 2003: Tellus B, v. 63, p. 1-22.

Keenan, T. F., D. Y. Hollinger, G. Bohrer, D. Dragoni, J. W. Munger, H. P. Schmid, and A. D. Richardson, 2013, Increase in forest water-use efficiency as atmospheric carbon dioxide concentrations rise: Nature, v. 499, p. 324-327.

Khatiwala, S., F. Primeau, and T. Hall, 2009, Reconstruction of the history of anthropogenic CO2 concentrations in the ocean: Nature, v. 462, p. 346-349.

889 Knorr, W., 2009, Is the airborne fraction of anthropogenic CO2 emissions increasing?: Geophysical
890 Research Letters, v. 36.
891 Landschützer, P., N. Gruber, D. Bakker, U. Schuster, S. Nakaoka, M. Payne, T. Sasse, and J. Zeng, 2013, A
892 neural network-based estimate of the seasonal to inter-annual variability of the Atlantic Ocean
893 carbon sink: Biogeosciences, v. 10.
894 Le Quéré, C., R. J. Andres, T. Boden, T. Conway, R. Houghton, J. I. House, G. Marland, G. P. Peters, G. van
895 der Werf, and A. Ahlström, 2013, The global carbon budget 1959–2011: Earth System Science
896 Data, v. 5, p. 165-185.
897 Le Quéré, C., M. R. Raupach, J. G. Canadell, G. Marland, L. Bopp, P. Ciais, T. J. Conway, S. C. Doney, R. A.
898 Feely, and P. Foster, 2009, Trends in the sources and sinks of carbon dioxide: Nature
899 Geoscience, v. 2, p. 831-836.
900 Le Quéré, C., C. Rödenbeck, E. T. Buitenhuis, T. J. Conway, R. Langenfelds, A. Gomez, C. Labuschagne, M.
901 Ramonet, T. Nakazawa, N. Metzl, N. Gillett, and M. Heimann, 2007, Saturation of the Southern
902 Ocean CO2 Sink Due to Recent Climate Change: Science, v. 316, p. 1735-1738.
903 Le Quéré, C., T. Takahashi, E. T. Buitenhuis, C. Rödenbeck, and S. C. Sutherland, 2010, Impact of climate
904 change and variability on the global oceanic sink of CO2: Global Biogeochemical Cycles, v. 24.
905 Lenton, A., B. Tilbrook, R. Law, D. Bakker, S. C. Doney, N. Gruber, M. Hoppema, M. Ishii, N. S. Lovenduski,
906 and R. J. Matear, 2013, Sea-air CO2 fluxes in the Southern Ocean for the period 1990–2009:
907 Biogeosciences Discussions, v. 10, p. 285-333.
908 Li, Z., D. Adamec, T. Takahashi, and S. C. Sutherland, 2005, Global autocorrelation scales of the partial
909 pressure of oceanic CO2: Journal of Geophysical Research: Oceans (1978–2012), v. 110.
910 Lovenduski, N. S., N. Gruber, S. C. Doney, and I. D. Lima, 2007, Enhanced CO2 outgassing in the Southern
911 Ocean from a positive phase of the Southern Annular Mode: Global Biogeochemical Cycles, v.
912 21.
913 Majkut, J. D., J. Sarmiento, and K. Rodgers, 2014, A growing oceanic carbon uptake: results from an
914 inversion study of surface pCO2 data: Global Biogeochemical Cycles, v. 28, p. 335-351.
915 Manning, A. C., and R. F. Keeling, 2006, Global oceanic and land biotic carbon sinks from the Scripps
916 atmospheric oxygen flask sampling network: Tellus B, v. 58, p. 95-116.
917 Marland, G., K. Hamal, and M. Jonas, 2009, How Uncertain Are Estimates of CO2 Emissions?: Journal of
918 Industrial Ecology, v. 13, p. 4-7.
919 Masarie, K. A., and P. P. Tans, 1995, Extension and integration of atmospheric carbon dioxide data into a
920 globally consistent measurement record: Journal of Geophysical Research: Atmospheres (1984–
921 2012), v. 100, p. 11593-11610.
922 Mast, M. A., J. T. Turk, D. W. Clow, and D. H. Campbell, 2011, Response of lake chemistry to changes in
923 atmospheric deposition and climate in three high-elevation wilderness areas of Colorado:
924 Biogeochemistry, v. 103, p. 27-43.
925 Matthews, R. B., M. van Noordwijk, E. Lambin, P. Meyfroidt, J. Gupta, L. Verchot, K. Hergoualc'h, and E.
926 Veldkamp, 2014, Implementing REDD+ (Reducing Emissions from Deforestation and
927 Degradation): evidence on governance, evaluation and impacts from the REDD-ALERT project:
928 Mitigation and Adaptation Strategies for Global Change, v. 19, p. 907-925.
929 Miller, J. B., P. P. Tans, and M. Gloor, 2014, Steps for success of OCO-2: Nature Geosci, v. 7, p. 691-691.
930 Nemani, R. R., C. D. Keeling, H. Hashimoto, W. M. Jolly, S. C. Piper, C. J. Tucker, R. B. Myneni, and S. W.
931 Running, 2003, Climate-driven increases in global terrestrial net primary production from 1982
932 to 1999: science, v. 300, p. 1560-1563.
933 Pan, Y., R. A. Birdsey, J. Fang, R. Houghton, P. E. Kauppi, W. A. Kurz, O. L. Phillips, A. Shvidenko, S. L.
934 Lewis, and J. G. Canadell, 2011, A large and persistent carbon sink in the world's forests: Science,
935 v. 333, p. 988-993.

936 Phillips, O. L., R. V. Martínez, L. Arroyo, T. R. Baker, T. Killeen, S. L. Lewis, Y. Malhi, A. M. Mendoza, D.
937 Neill, and P. N. Vargas, 2002, Increasing dominance of large lianas in Amazonian forests: Nature,
938 v. 418, p. 770-774.
939 Pongratz, J., C. Reick, R. Houghton, and J. House, 2014, Terminology as a key uncertainty in net land use
940 and land cover change carbon flux estimates: Earth System Dynamics, v. 5, p. 177-195.
941 Poulter, B., D. Frank, P. Ciais, R. B. Myneni, N. Andela, J. Bi, G. Broquet, J. G. Canadell, F. Chevallier, and
942 Y. Y. Liu, 2014, Contribution of semi-arid ecosystems to interannual variability of the global
943 carbon cycle: Nature, v. 509, p. 600-603.
944 Raupach, M., C. Le Quéré, G. Peters, and J. Canadell, 2013, Anthropogenic CO2 emissions: Nature
945 Climate Change, v. 3, p. 603-604.
946 Reichstein, M., M. Bahn, P. Ciais, D. Frank, M. D. Mahecha, S. I. Seneviratne, J. Zscheischler, C. Beer, N.
947 Buchmann, and D. C. Frank, 2013, Climate extremes and the carbon cycle: Nature, v. 500, p. 287-
948 295.
949 Riebesell, U., K. G. Schulz, R. Bellerby, M. Botros, P. Fritsche, M. Meyerhöfer, C. Neill, G. Nondal, A.
950 Oschlies, and J. Wohlers, 2007, Enhanced biological carbon consumption in a high CO2 ocean:
951 Nature, v. 450, p. 545-548.
952 Rödenbeck, C., R. Keeling, D. Bakker, N. Metzl, A. Olsen, C. Sabine, and M. Heimann, 2013, Global
953 surface-ocean p (CO2) and sea-air CO2 flux variability from an observation-driven ocean mixed-
954 layer scheme.
955 Sarmiento, J. L., M. Gloor, N. Gruber, C. Beaulieu, A. R. Jacobson, S. E. Mikaloff Fletcher, S. Pacala, and K.
956 Rodgers, 2010, Trends and regional distributions of land and ocean carbon sinks:
957 Biogeosciences, v. 7, p. 2351-2367.
958 Schuster, U., and A. J. Watson, 2007, A variable and decreasing sink for atmospheric CO2 in the North
959 Atlantic: Journal of Geophysical Research: Oceans (1978–2012), v. 112.
960 Stocker, B., K. Strassmann, and F. Joos, 2011, Sensitivity of Holocene atmospheric CO 2 and the modern
961 carbon budget to early human land use: analyses with a process-based model: Biogeosciences,
962 v. 8.
963 Takahashi, T., S. C. Sutherland, and A. Kozyr, 2014, Global Ocean Surface Water Partial Pressure of CO_2
964 Database: Measurements Performed During 1957-2013 (Version 2013), **O**RNL/CDIAC-160, NDP-
965 088(V2012). Carbon Dioxide Information Analysis Center, **O**ak Ridge National Laboratory, U.S.
966 Department of Energy, Oak Ridge, Tennessee.
967 Thoning, K. W., P. P. Tans, and W. D. Komhyr, 1989, Atmospheric carbon dioxide at Mauna Loa
968 Observatory: 2. Analysis of the NOAA GMCC data, 1974–1985: Journal of Geophysical Research:
969 Atmospheres (1984–2012), v. 94, p. 8549-8565.
970 View-CO2, G., 2013, *Cooperative Global Atmospheric Data Integration Project. 2013, updated annually.*
971 *Multi-laboratory compilation of synchronized and gap-filled atmospheric carbon dioxide records*
972 *for the period 1979-2012*, Compiled by NOAA Global Monitoring Division: Boulder, Colorado,
973 U.S.A.
974 Wanninkhof, R., G.-H. Park, T. Takahashi, C. Sweeney, R. Feely, Y. Nojiri, N. Gruber, S. C. Doney, G. A.
975 McKinley, and A. Lenton, 2013, Global ocean carbon uptake: magnitude, variability and trends:
976 Biogeosciences, v. 10.
977 Yang, X., T. Richardson, and A. Jain, 2010, Contributions of secondary forest and nitrogen dynamics to
978 terrestrial carbon uptake: Biogeosciences Discussions, v. 7.
979 Zhao, M., and S. W. Running, 2010, Drought-induced reduction in global terrestrial net primary
980 production from 2000 through 2009: science, v. 329, p. 940-943.

981

982

983

984 Tables and Figures

985 Table 1. Decadal changes in variables of the global C budget. Reported are decadal means for the
986 atmospheric growth rate, land use emissions, fossil fuel emissions, global uptake, the Airborne Fraction,
987 Net Ocean Uptake, and Net Land Uptake. The first number below the mean (in parentheses) is the
988 mean of the decadal standard deviations that provides a measure of our ability to detect a change in
989 that variable. The second number below the meane (in parentheses) is the standard deviation of the
990 decadal means that provides a measure of variance in that variable.

	Decadal Mean Values and Standard Deviations.				
Variable	1960s	1970s	1980s	1990s	2000s
Atmospheric CO_2 (PgC yr^{-1};∂C/∂t)	1.75	2.72	3.42	3.18	4.14
mean of standard deviations	(0.60)	(0.61)	(0.22)	(0.18)	(0.16)
standard deviation of the means	(0.61)	(0.91)	(1.21)	(1.40)	(0.82)
Land Use Emissions (PgC yr^{-1};E_L)	1.16	1.28	1.42	1.15	0.89
mean of standard deviations	(0.76)	(0.64)	(0.65)	(0.67)	(0.63)
standard deviation of the means	(0.25)	(0.11)	(0.13)	(0.23)	(0.12)
Fossil Fuel Emissions (PgC yr^{-1};E_F)	3.09	4.76	5.53	6.45	7.89
mean of standard deviations	(0.15)	(0.24)	(0.30)	(0.35)	(0.47)
standard deviation of the means	(0.44)	(0.41)	(0.33)	(0.24)	(0.69)
Net Global Uptake (PgC yr^{-1}; ΣN)	-2.51	-3.32	-3.61	-4.38	-4.64
mean of standard deviations	(0.83)	(0.76)	(0.52)	(0.56)	(0.50)
standard deviation of the means	(0.52)	(0.84)	(1.13)	(1.37)	(0.98)
Airborne Fraction (AF)	0.42	0.45	0.48	0.42	0.47
mean of standard deviations	(0.16)	(0.11)	(0.05)	(0.04)	(0.03)
standard deviation of the means	(0.12)	(0.14)	(0.16)	(0.18)	(0.10)
Net Ocean Uptake (PgC yr^{-1}; N_O)	-1.11	-1.43	-1.79	-2.07	-2.21
mean of standard deviations	(1.31)	(1.32)	(1.33)	(1.35)	(1.39)
standard deviation of the means	(0.24)	(0.16)	(0.06)	(0.09)	(0.19)
Net Land Uptake (PgC yr^{-1}; N_L)	-1.39	-1.89	-1.78	-2.35	-2.46
mean of standard deviations	(1.56)	(1.51)	(1.43)	(1.46)	(1.43)
standard deviation of the means	(0.56)	(0.90)	(1.17)	(1.48)	(1.06)

991

992

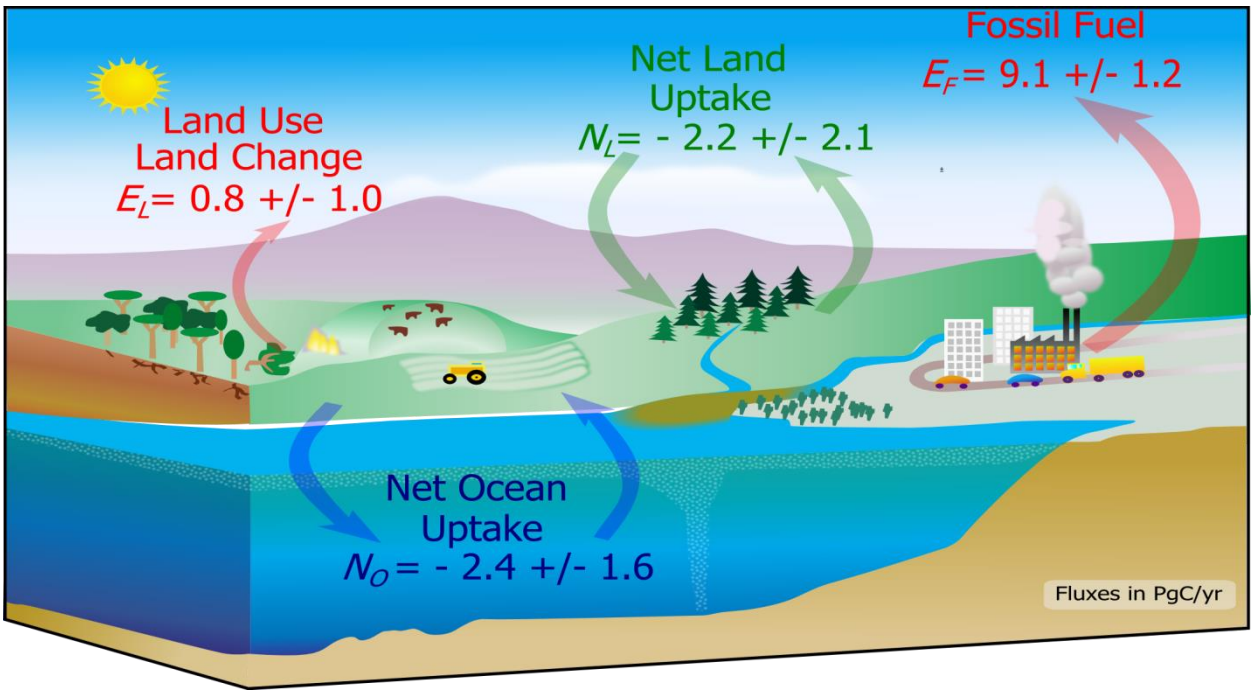

Figure 1. Diagram of the global carbon budget in the year 2010. Major fluxes of C to the atmospheric reservoir of CO_2 are from fossil fuel emissions (F_F) and land-use land conversion (F_L) and are illustrated as red vectors. Net land (N_L) uptake of C from the reservoir of atmospheric CO_2 is illustrated by green vectors and net ocean uptake (N_O) is illustrated by blue vectors. The size of the vectors are proportional to the mass flux of C as indicated inpetagrams of C per year, where 1 Pg = 10^{15} g (illustration modified from Wikimedia Commons). Error estimates for each flux in 2010 are expressed as ± 2 σ.

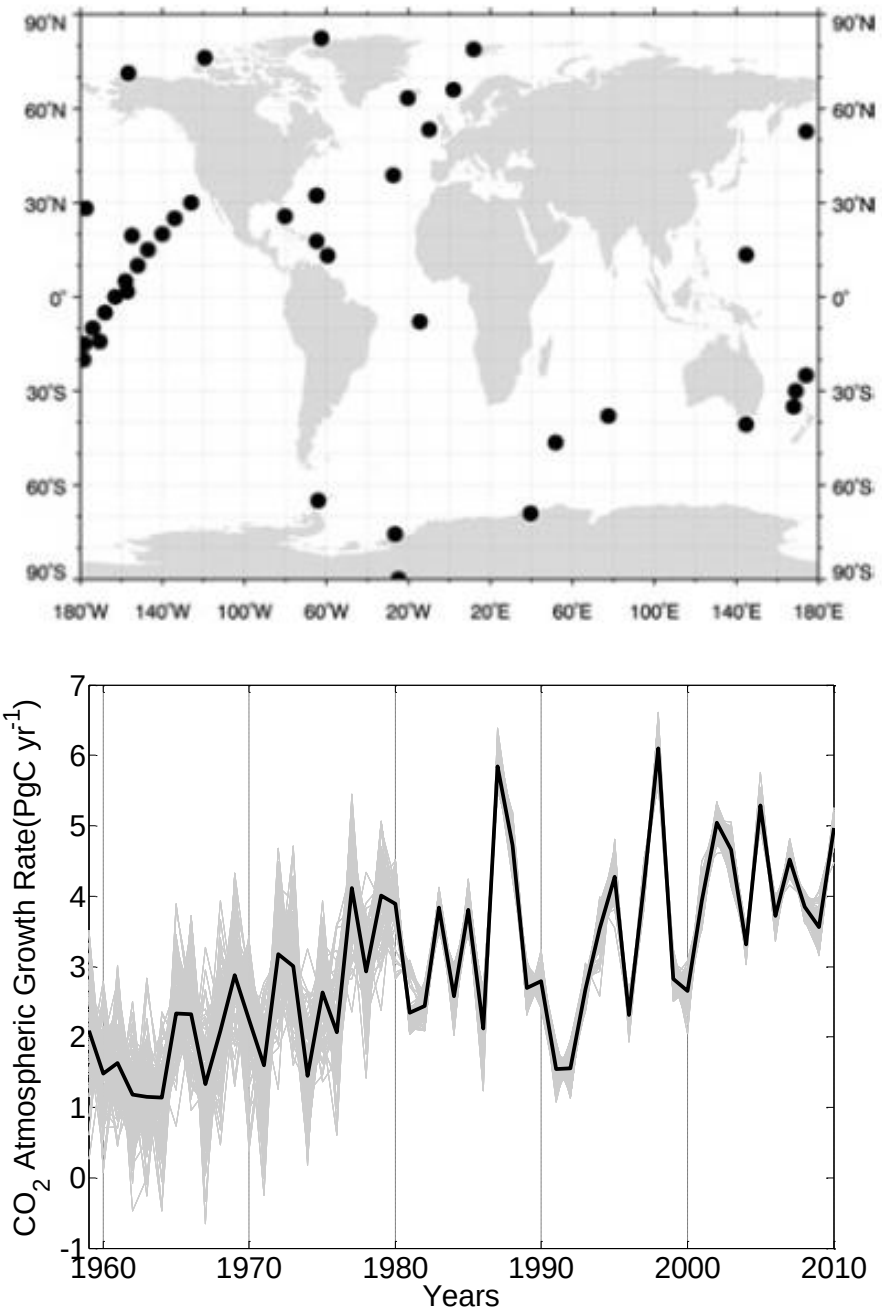

Figure 2. The global observation network used in calculating the annual atmospheric CO_2 growth rate. The annual growth rate of atmospheric CO_2 is calculated from re-sampling sites in the global network located in the marine boundary layer (black points; top panel). The annual growth rate since 1980 is calculated from the entire marine boundary layer, while the growth rate prior to 1980 is calculated from observation sites at Mauna Loa, Hawaii, USA and South Pole, Antarctica. The mean atmospheric growth rate is illustrated as a thick black line and growth rates calculated from the 100 simulated sampling networks are illustrated by the thin grey traces.

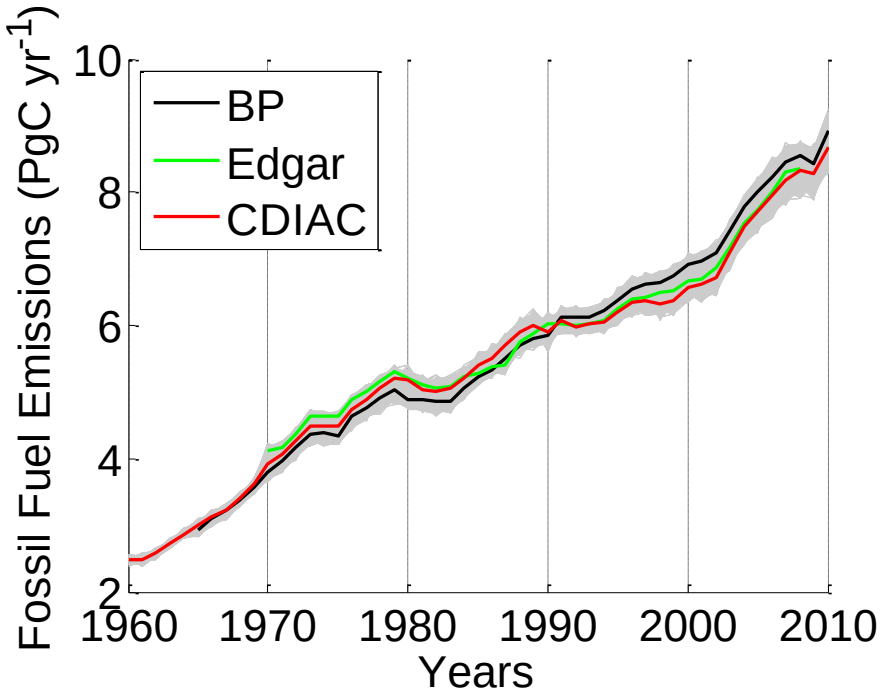

1013

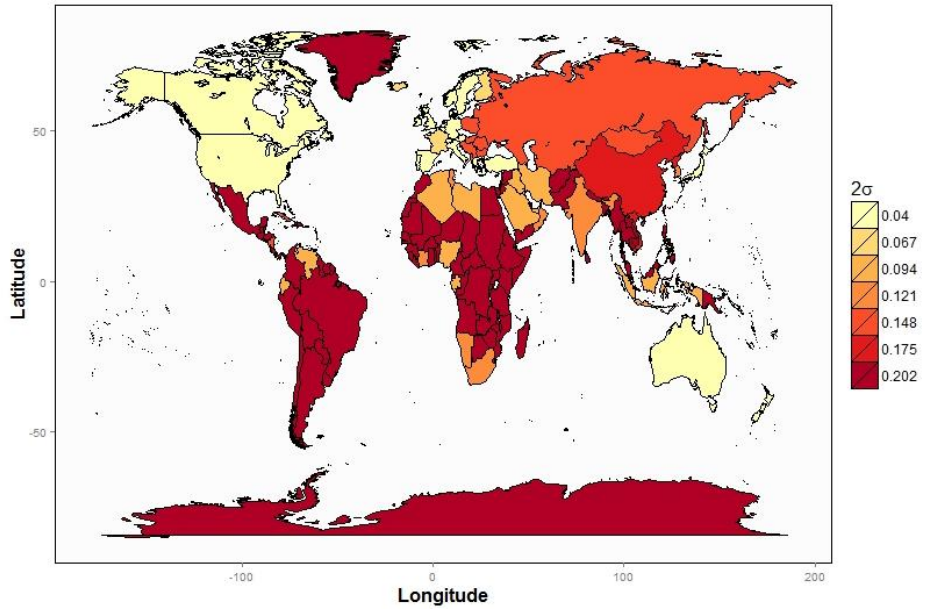

1014

1015 Figure 3. Fossil fuel emission estimates and their errors from 1960 to 2010. The three inventories (top
1016 panel) compared are from BP (aka British Petroleum; black), the Emission Database for Global
1017 Atmospheric Research (EDGAR: green), and the Carbon Dioxide Information and Analysis Center (CDIAC;
1018 red). All inventories also include cement production. Thin grey traces represent the Monte-Carlo
1019 simulations of uncertainty for the fossil fuel emission inventories (N = 3 x 500= 1500). Errors are
1020 estimated by deriving regional error distributions and then randomly drawing from these distributions
1021 for error estimates of individual nations (bottom panel) where error estimates are taken from (Andres et
1022 al., 2014a). Emission errors are reported as relative errors of total emissions by nation and emission
1023 errors for Antarctica are for the Antarctic fishing fleet. See supplemental table 1 for national errors.

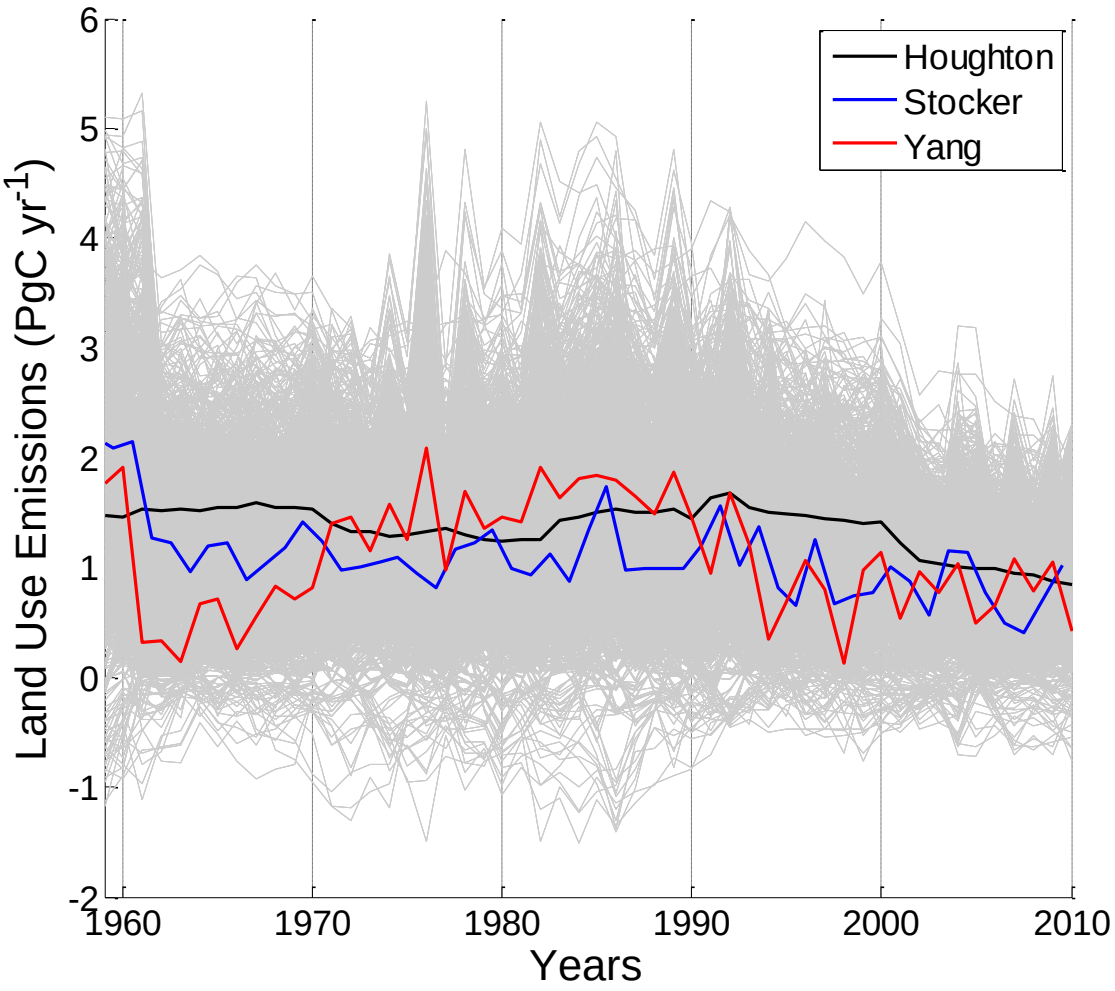

1024

1025 Figure 4. Comparison of land use land change emission inventories from 1960 to 2010. The three
1026 inventories compared are the bookkeeping approach (Houghton et al. 2012; black), model derived
1027 estimates including historical land use (Stocker et al 2013: blue), and model derived estimates, including
1028 historical land use and nitrogen cycling (Yang et al 2010; red). Thin grey traces represent the Monte-
1029 Carlo simulations of uncertainty for the land use emission estimates (N = 3 x 500= 1500).

1030

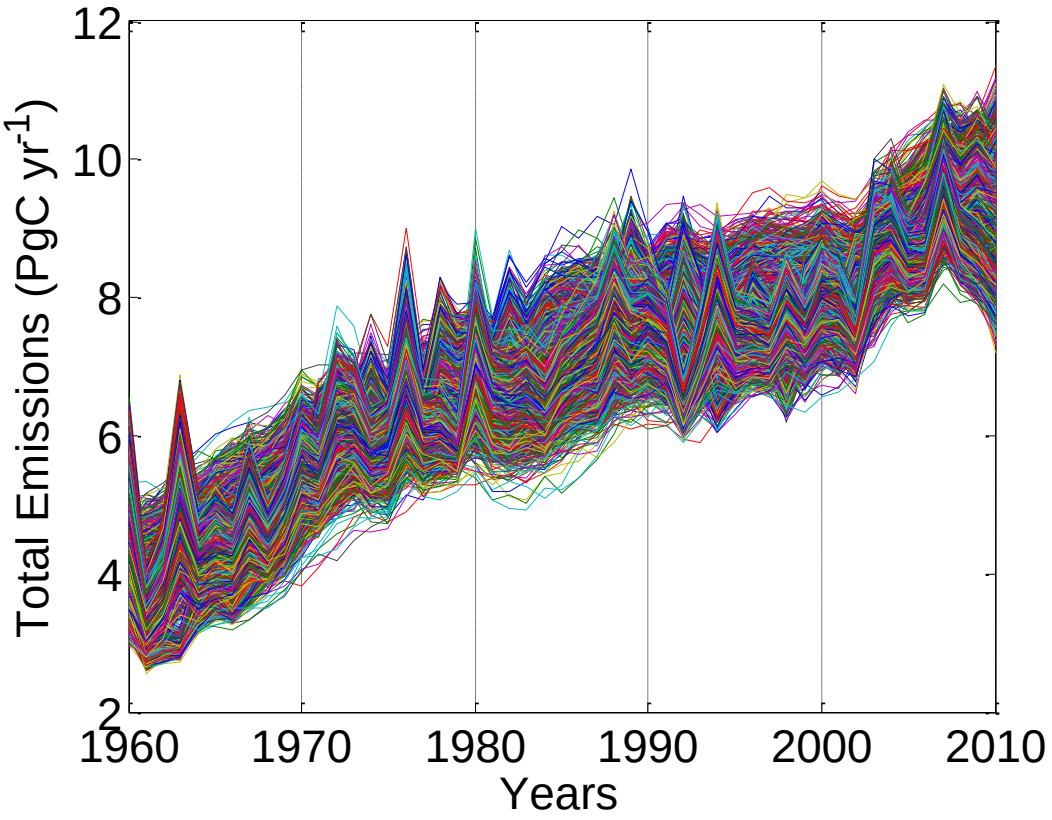

Figure 5. Total emission scenarios including uncertainty. Plotted are all combinations of the sum of land use and fossil fuel emission estimates included in this study A total of 500 realizations for each of the 3 land use emission estimates and each of the fossil fuel emission estimates is included for a total of 4500 global emission realizations (each colored line).

1037

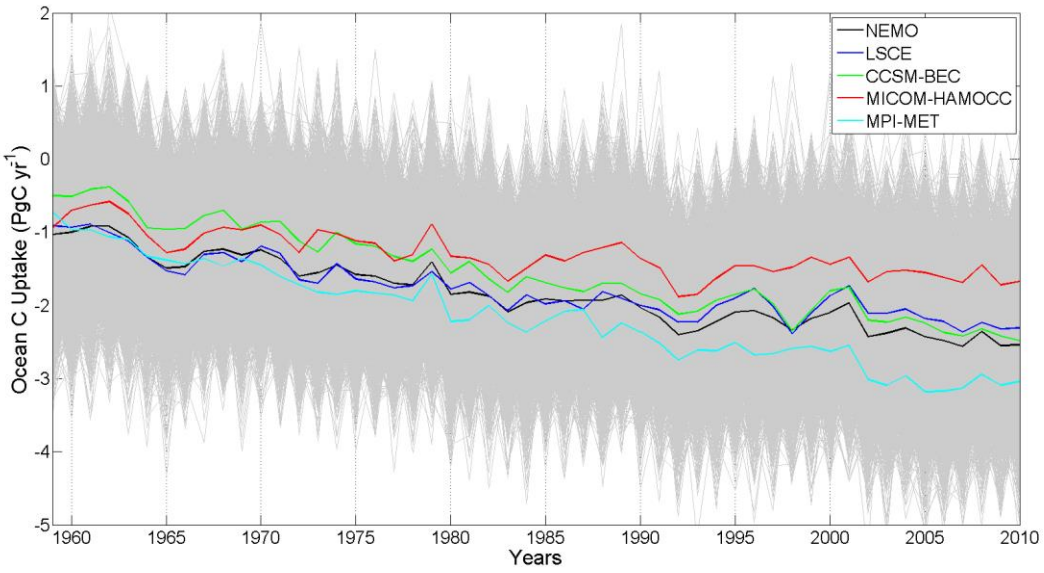

1038

1039 Figure 6. Ocean carbon uptake estimates from five different ocean biogeochemical models.
1040 Independent time invariant random error of 1.3 PgC (2 σ) has been added to each annual model
1041 simulation according to independent estimates of ocean C uptake (Ishidoya et al. 2012). For each
1042 biogeochemical model estimate 900 Monte-Carlo simulations were performed to better estimate error
1043 (thin grey lines).

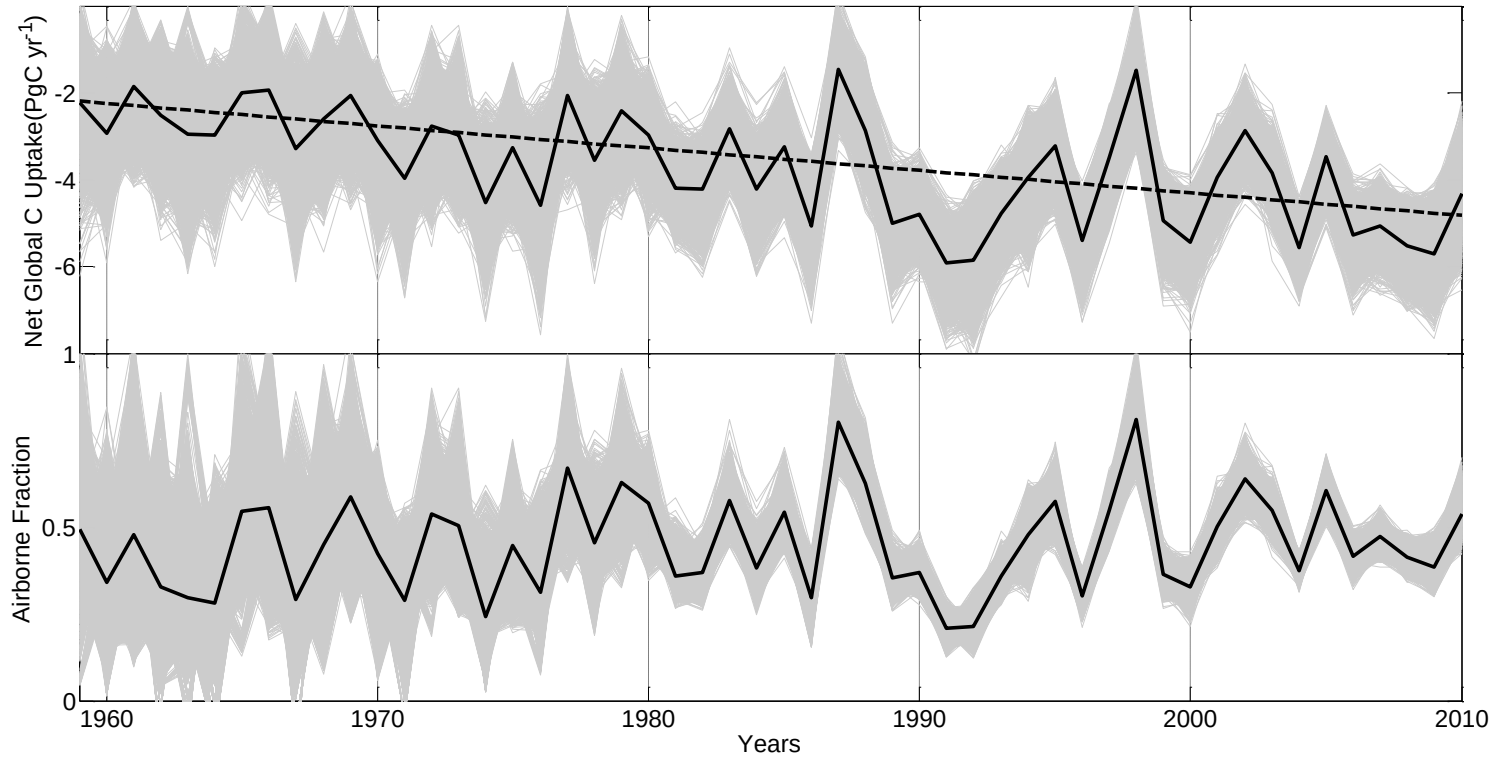

Figure 7. Simulations of net global C uptake and the airborne fraction from 1959 to 2010. Net global C uptake (*ΣN*; top panel) is plotted in comparison to the airborne fraction (*AF*; bottom panel). A total of 4500 simulations of *ΣN* and *AF* are plotted in each panel (thin grey lines) and mean annual values overlaid (thick black line). A significant acceleration in global net C uptake is indicated by the dashed line with a slope = -0.05 PgC yr^{-2} and a p-value = 5.5 x 10^{-5} fitted to the annual mean *ΣN* values. See supplemental table 2 for global C uptake values and their uncertainty.

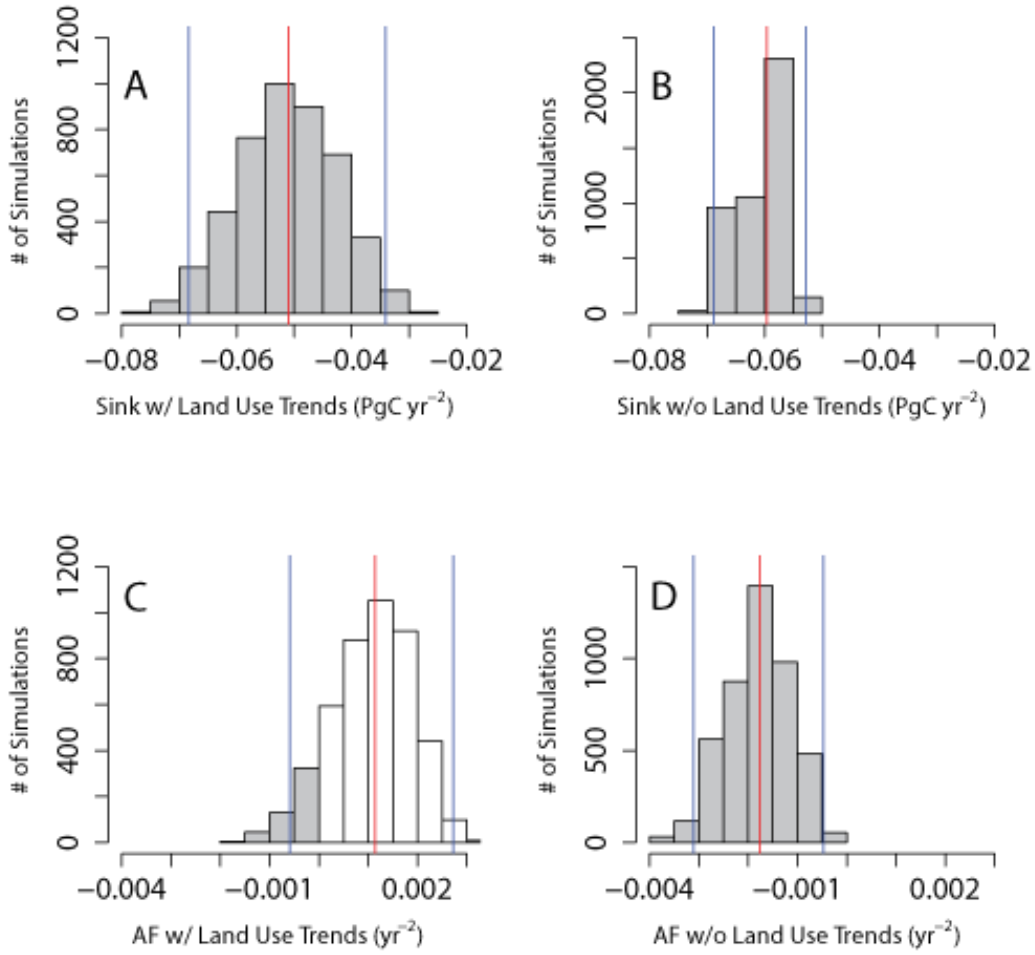

Figure 8. Trends in global carbon uptake. Plotted are the histograms of slopes fitted to 4500 simulations of net global carbon uptake (i.e. global sink ΣN in panels A and B) and the airborne fraction (i.e. AF in panels C and D). Plotted also are the slopes fitted to 4500 simulations without land use emissions included for ΣN (B) and AF (C). Negative trend slopes (grey filled bars) of ΣN indicate accelerating net global C uptake, whereas positive slopes (open bars) of AF indicate a decrease in relative C uptake efficiency. The median slope values are overlaid (red lines) for comparison with the 2 σ trend calculations (blue lines).

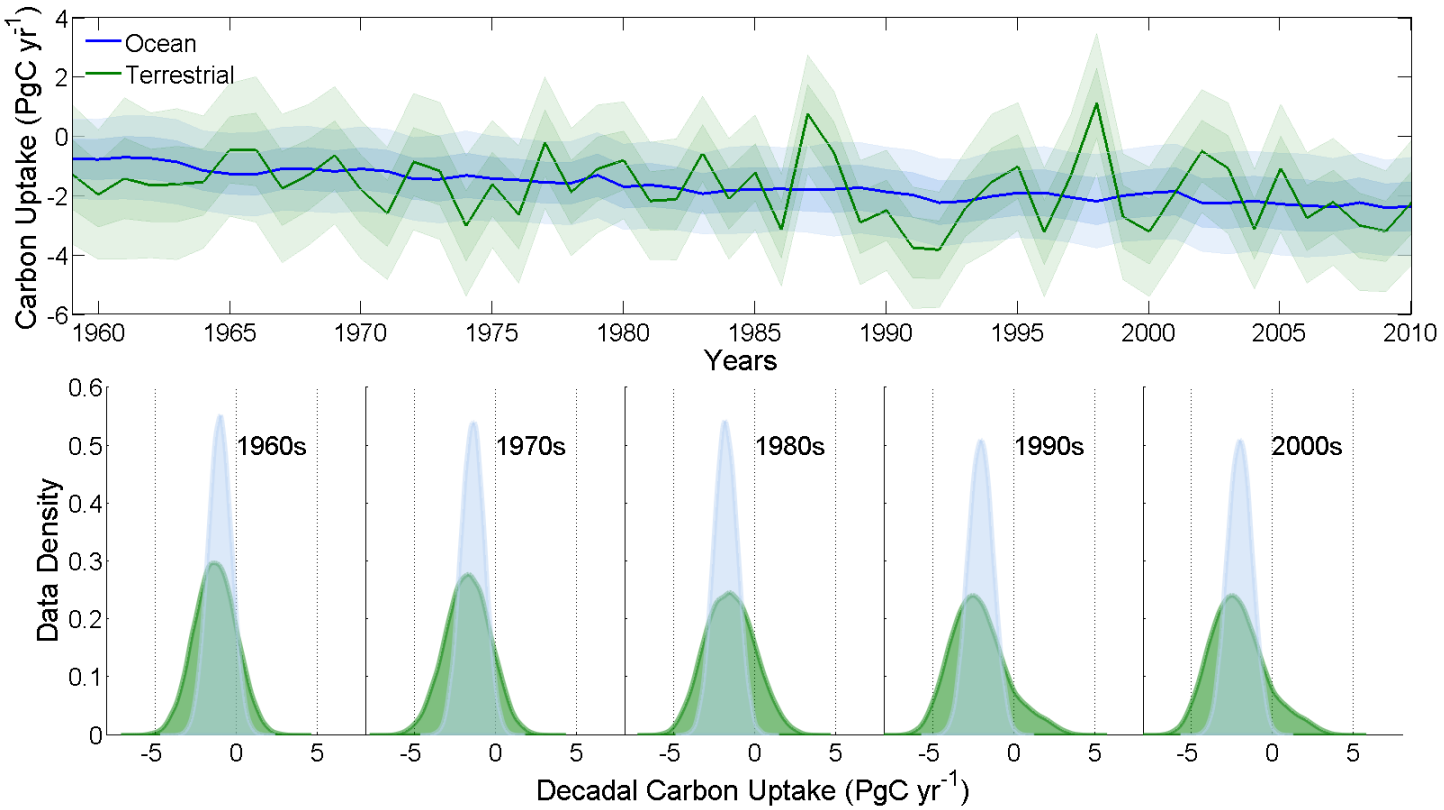

Figure 9. Trends in global carbon uptake by the land and ocean. Both the land (green line) and ocean (blue line) show increasing carbon uptake over the last 50 years as evidenced by increasingly negative uptake values (top panel). Confidence intervals represent the 1σ (dark transparent) and 2σ (light transparent) distribution about the mean values for the land (green line) and the ocean (blue line). Kernel density functions for the distribution of uptake by the land (green) and ocean (blue) by decades (bottom panel) showing the increase in C uptake by decade but also the increase in variance for land C uptake. See supplemental table 2 for ocean and terrestrial C uptake values and their uncertainty.

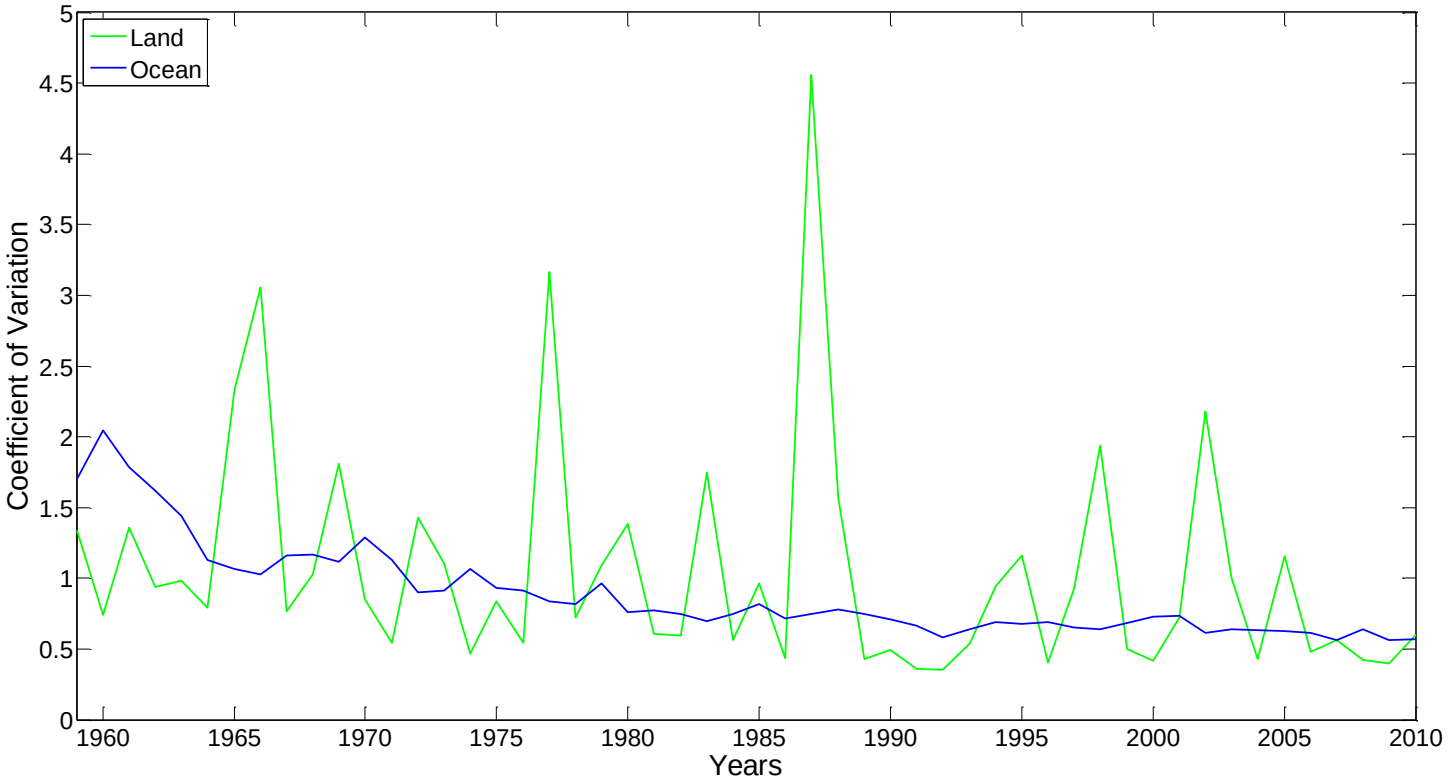

Figure 10. Coefficient of variation for net land and ocean C uptake for each year from 1959 to 2010. Coefficients of variation (CV) were calculated as the standard deviation/mean from each of our 4500 simulations of annual uptake. Values of CV for net land uptake (green) are compared with values of CV for net ocean uptake (blue). Absolute mean values were used to account for changes in sign of net land uptake that occurred over the 50 year period.

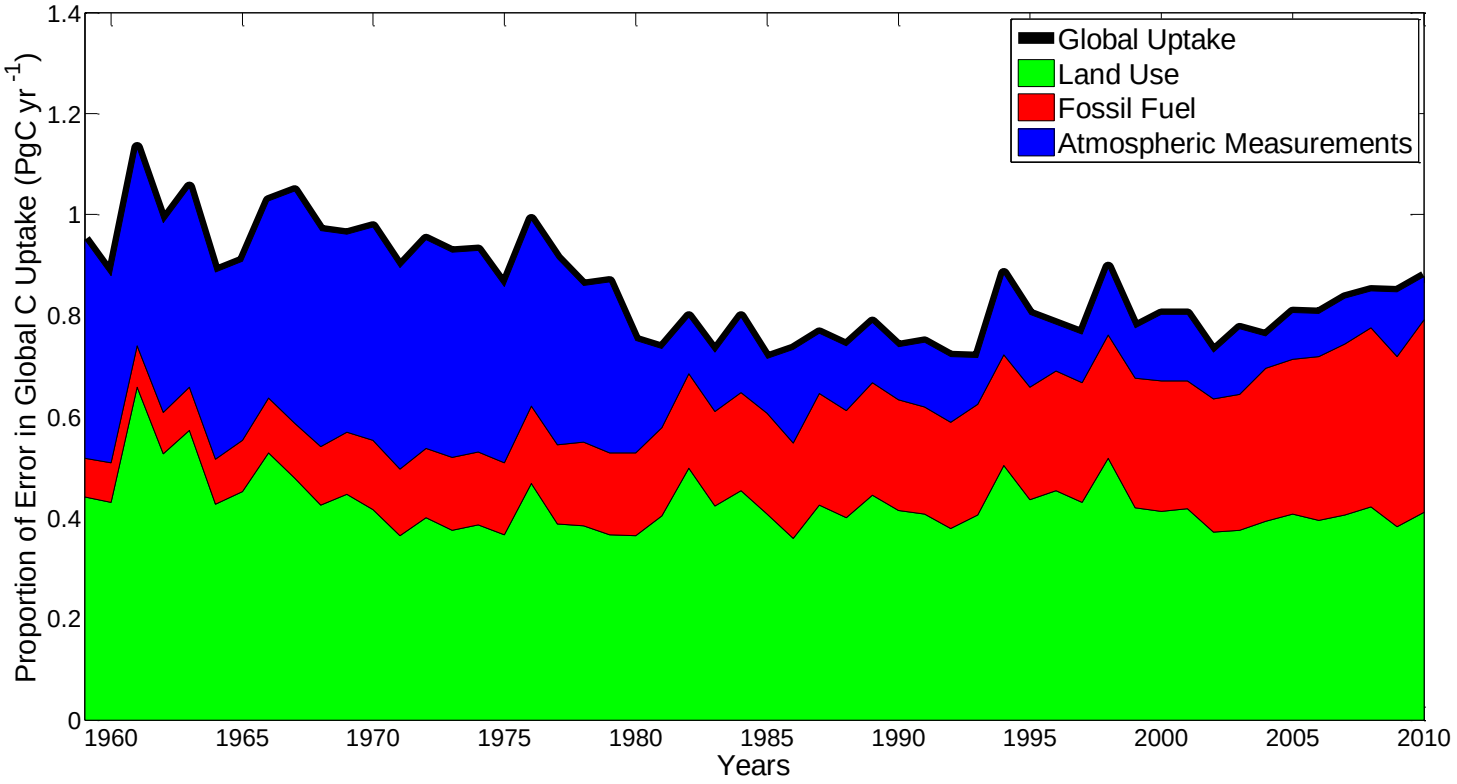

Figure 11. Proportion of error in terms contributing to the global carbon uptake. The total error in global C uptake is calculated as the square root sum of squared standard deviations for each term in the global budget (black line). The proportion of global C uptake uncertainty contributed from land use (green area) has remained fairly constant, the proportion of global C uptake uncertainty contributed from fossil fuels (red area) has risen in recent years, and the proportion of global C uptake uncertainty contributed from atmospheric CO_2 measurements (blue area) has decreased.